

# Tacrolimus-resistant SARS-CoV-2-specific T cell products to prevent and treat severe COVID-19 in immunosuppressed patients

Lena Peter,<sup>1,2</sup> Désirée Jacqueline Wending,<sup>1</sup> Stephan Schlickeiser,<sup>1,4</sup> Henrike Hoffmann,<sup>3</sup> Rebecca Noster,<sup>1</sup> Dimitrios Laurin Wagner,<sup>1,3,4,5</sup> Ghazaleh Zarrinrad,<sup>1,2,3</sup> Sandra Münch,<sup>3</sup> Samira Picht,<sup>1</sup> Sarah Schulenberg,<sup>1,2</sup> Hanieh Moradian,<sup>1,6,7</sup> Mir-Farzin Mashreghi,<sup>1,8</sup> Oliver Klein,<sup>1</sup> Manfred Gossen,<sup>1,6</sup> Toralf Roch,<sup>1,4,9</sup> Nina Babel,<sup>1,4,9</sup> Petra Reinke,<sup>1,3</sup> Hans-Dieter Volk,<sup>1,3,4</sup> Leila Amini,<sup>1,3,10</sup> and Michael Schmueck-Henneresse<sup>1,3,10</sup>

<sup>1</sup>Berlin Institute of Health (BIH) at Charité – Universitätsmedizin Berlin, BIH Center for Regenerative Therapies (BCRT), Charitéplatz 1, 10117 Berlin, Germany; <sup>2</sup>Einstein Center for Regenerative Therapies at Charité – Universitätsmedizin Berlin, Augustenburger Platz 1, 13353 Berlin, Germany; <sup>3</sup>Berlin Center for Advanced Therapies (BeCAT) at Charité – Universitätsmedizin Berlin, Augustenburger Platz 1, 13353 Berlin, Germany; <sup>4</sup>Charité – Universitätsmedizin Berlin, corporate member of Freie Universität Berlin and Humboldt-Universität zu Berlin, Institute of Medical Immunology, Augustenburger Platz 1, 13353 Berlin, Germany; <sup>5</sup>Charité – Universitätsmedizin Berlin, corporate member of Freie Universität Berlin and Humboldt-Universität zu Berlin, Institute of Transfusion Medicine, Charitéplatz 1, 10117 Berlin, Germany; <sup>6</sup>Institute of Active Polymers, Helmholtz-Zentrum Hereon, Kantstr. 55, 14513 Teltow, Germany; <sup>7</sup>Institute of Biochemistry and Biology, University of Potsdam, Karl-Liebknecht-Str. 24-25, 14476 Potsdam, Germany; <sup>8</sup>Deutsches Rheuma-Forschungszentrum Berlin, a Leibniz Institute, Charitéplatz 1, 10117 Berlin, Germany; <sup>9</sup>Center for Translational Medicine, Immunology, and Transplantation, Medical Department I, Marien Hospital Herne, University Hospital of the Ruhr-University Bochum, Hölkeskampring 40, 44625 Herne, Germany

**Solid organ transplant (SOT) recipients receive therapeutic immunosuppression that compromises their immune response to infections and vaccines. For this reason, SOT patients have a high risk of developing severe coronavirus disease 2019 (COVID-19) and an increased risk of death from severe acute respiratory syndrome coronavirus-2 (SARS-CoV-2) infection. Moreover, the efficiency of immunotherapies and vaccines is reduced due to the constant immunosuppression in this patient group. Here, we propose adoptive transfer of SARS-CoV-2-specific T cells made resistant to a common immunosuppressant, tacrolimus, for optimized performance in the immunosuppressed patient. Using a ribonucleoprotein approach of CRISPR-Cas9 technology, we have generated tacrolimus-resistant SARS-CoV-2-specific T cell products from convalescent donors and demonstrate their specificity and function through characterizations at the single-cell level, including flow cytometry, single-cell RNA (scRNA) Cellular Indexing of Transcripts and Epitopes (CITE), and T cell receptor (TCR) sequencing analyses. Based on the promising results, we aim for clinical validation of this approach in transplant recipients. Additionally, we propose a combinatory approach with tacrolimus, to prevent an overshooting immune response manifested as bystander T cell activation in the setting of severe COVID-19 immunopathology, and tacrolimus-resistant SARS-CoV-2-specific T cell products, allowing for efficient clearance of viral infection. Our strategy has the potential to prevent severe COVID-19 courses in SOT or autoimmunity settings and to prevent immunopathology while providing viral clearance in severe non-transplant COVID-19 cases.**

## INTRODUCTION

Severe acute respiratory syndrome coronavirus 2 (SARS-CoV-2) emerged in 2019, causing respiratory tract disorders, referred to as coronavirus disease 2019 (COVID-19), and led to a worldwide pandemic.<sup>1,2</sup> While, in the general population, most SARS-CoV-2 infections show a mild disease course, severe COVID-19 is more common among individuals under chronic immunosuppression, such as transplant recipients, autoimmune patients,<sup>3,4</sup> and the elderly.<sup>5</sup> Chronic immunosuppression increases susceptibility to respiratory viral infections, which are increasingly recognized to be a major cause of morbidity and mortality among transplant recipients.<sup>3,6–8</sup>

Recent studies suggest that SOT recipients are at high risk for complications or death due to SARS-CoV-2 infection.<sup>3,9–13</sup> In a large US cohort (1,925) of SARS-CoV-2<sup>+</sup> SOT recipients, 42.9% of SOT recipients with SARS-CoV-2 had to be hospitalized and the infection was

Received 16 February 2022; accepted 25 February 2022;  
<https://doi.org/10.1016/j.omtm.2022.02.012>.

<sup>10</sup>These authors contributed equally

**Correspondence:** Leila Amini, PhD, Berlin Institute of Health (BIH) at Charité – Universitätsmedizin Berlin, BIH Center for Regenerative Therapies (BCRT) and BeCAT at Charité – Universitätsmedizin Berlin, Augustenburger Platz 1, 13353 Berlin, Germany.  
**E-mail:** [leila.amini@bih-charite.de](mailto:leila.amini@bih-charite.de)

**Correspondence:** Michael Schmueck-Henneresse, PhD, Berlin Institute of Health (BIH) at Charité – Universitätsmedizin Berlin, BIH Center for Regenerative Therapies (BCRT) and BeCAT at Charité – Universitätsmedizin Berlin, Augustenburger Platz 1, 13353 Berlin, Germany.  
**E-mail:** [michael.schmueck-henneresse@bih-charite.de](mailto:michael.schmueck-henneresse@bih-charite.de)



associated with increased risk for acute kidney injury, organ rejection, graft failure, and major cardiologic problems.<sup>14</sup> Furthermore, current findings indicate that immunosuppressed and elderly patients mount weak responses to COVID-19 vaccines. Consequently, vaccination in these populations may not provide protection against severe SARS-CoV-2 infections or to emerging novel SARS-CoV-2 strains, leaving them at risk.<sup>15–20</sup> Indeed, initial studies reported that, despite being vaccinated, SOT patients still became infected with SARS-CoV-2 and required hospitalization, highlighting the necessity of novel strategies to protect this vulnerable population.<sup>21–23</sup>

SARS-CoV-2-specific T cells have been detected in convalescent patients in multiple studies, indicating an important role for T cells in viral clearance and development of protective immunity.<sup>24–26</sup> Thus, SARS-CoV-2-specific adoptive T cell therapy (ACT) has been suggested as an early treatment or preventive strategy for COVID-19 in immunocompromised or immunosuppressed individuals<sup>27</sup> as well as more generally for treatment of acute COVID-19.<sup>28,29</sup> Virus-specific ACT has already been administered with a very low incidence of adverse effects to prevent and treat infections in patients after hematopoietic stem cell transplantation and SOT.<sup>30–32</sup> Furthermore, recent studies have shown the feasibility of generating SARS-CoV-2-specific T cell products (TCPs) from the blood of patients who have recovered from SARS-CoV-2 infection.<sup>27,28</sup> Clinical trials are now needed to demonstrate safety, efficiency, and persistence of antiviral TCPs *in vivo* and to determine any therapeutic benefit of ACT for COVID-19 patients. However, current ACT strategies may not benefit COVID-19 patients who are also treated with immunosuppressants, which includes SOT recipients. They might, however, benefit from adoptive transfer of immunosuppression-resistant SARS-CoV-2-specific TCPs, allowing prevention of overshooting immune responses while maintaining some form of viral anti-immunity. Additionally, reported data imply that ACT enhances induction of antibody responses,<sup>33</sup> thus immunosuppression-resistant adoptive SARS-CoV-2-specific ACT may help to establish protective immunity, consisting of both T and B cell responses,<sup>34,35</sup> in immunosuppressed patients, who often fail to mount protective long-term antibody responses after vaccination.<sup>17–20</sup>

Immunosuppression-resistant adoptive SARS-CoV-2-specific ACT could also be beneficial beyond immunosuppressed patient populations. Severe COVID-19 is associated with extrapulmonary systemic hyperinflammation syndrome characterized by an overshooting innate and adaptive immune response (sometimes referred to as cytokine storm) that further results in tissue damage and multi-organ failure.<sup>36,37</sup> Studies indicate that dysregulated T cell function contributes to COVID-19-associated hyperinflammation and impaired viral clearance.<sup>38–42</sup> Consequently, immunosuppressive corticosteroids are currently the first line of treatment for patients with severe COVID-19-associated hyper-inflammation<sup>43,44</sup> and can reduce mortality in patients requiring respiratory support.<sup>45</sup> However, their generalized use in treating coronavirus diseases has been controversial: some reports suggest improved disease outcomes in COVID-19 patients upon corticosteroid treatment,<sup>43,44,46</sup> while others suggest corticosteroids prolong the duration of hospitalization and delay viral elimination.<sup>47–50</sup> Thus,

there is an urgent need for effective and safe strategies aiming to support viral clearance while preventing SARS-CoV-2-associated hyperinflammation and tissue damage in patients with severe COVID-19.

The calcineurin inhibitor (CNI) tacrolimus (Tac) may be an attractive alternative to corticosteroids. Tac is reported to inhibit proinflammatory cytokine production and the replication of human coronavirus (HCoV) SARS-CoV-1, HCoV-NL63, and HCoV-229E,<sup>51,52</sup> to reduce T cell-associated hyperinflammation, and to have protective effects in SOT patients infected with Middle East respiratory syndrome coronavirus (MERS-CoV) or SARS-CoV-2.<sup>53–56</sup> Indeed, Tac combined with prednisolone (Pred) pulses ([ClinicalTrials.gov Identifier: NCT04341038](https://clinicaltrials.gov/ct2/show/study/NCT04341038))<sup>57</sup> and the CNI, cyclosporine A (CsA),<sup>58</sup> are under investigation for treatment of COVID-19 in clinical trials. However, reports imply that immunosuppressed transplant recipients under Tac therapy also show prolonged viral shedding upon SARS-CoV-2 infection, illustrating the need for regeneration of specific immune responses to SARS-CoV-2 in these patients.<sup>59–62</sup> The feasibility of generating glucocorticoid-resistant SARS-CoV-2-specific T cells for ACT has recently been described<sup>29</sup>; however, as tacrolimus is required to prevent organ rejection after SOT transplantation and additionally is reported to support antiviral and anti-inflammatory processes toward coronavirus infections,<sup>51–56</sup> it might be an attractive alternative to corticosteroid-based immunosuppression to reduce or prevent COVID-19-associated hyperinflammation. Thus, we suggest combination therapy for severe COVID-19 using Tac to prevent immunopathology, combined with tacrolimus-resistant adoptive antiviral T cell therapy to improve viral control as a novel treatment concept, both for immunocompromised SOT patients as well as in severe non-transplant COVID-19 cases.<sup>63</sup>

We report the feasibility of generating SARS-CoV-2-specific Tac-resistant antiviral T cells suitable for ACT from convalescent SARS-CoV-2-infected individuals utilizing our vector-free gene-editing approach targeting *FKBP12*, which codes for the adapter protein required for the immunosuppressive function of Tac in antiviral T cells.<sup>63,64</sup> Functional analysis confirmed that *FKBP12* KO SARS-CoV-2-specific T cells are highly resistant to Tac treatment, maintaining their effector function as measured by antigen-specific cytokine production. In contrast, the antiviral cytokine production of these novel *FKBP12* KO SARS-CoV-2-specific T cells was efficiently suppressed by *FKBP12*-independent immunosuppression via the alternative CNI, CsA. We thus provide an inherent safety switch in case of potential adverse effects of *FKBP12* KO T cells *in vivo*.<sup>43</sup> Our GMP-compatible manufacturing process allows for clinical-grade production of these innovative Tac-resistant TCPs as a pre-requisite for a first-in-human clinical trial investigating the potential of SARS-CoV-2-specific *FKBP12* KO T cells in transplant recipients.

## RESULTS

### SARS-CoV-2-specific T cells from SARS-CoV-2<sup>+</sup> convalescent donors predominantly target the nucleocapsid and spike proteins

To assess the feasibility of isolating SARS-CoV-2-reactive T cells, we analyzed the antiviral T cell responses to SARS-Cov-2 structural and

accessory proteins in individuals with a history of asymptomatic or mild SARS-CoV-2 infection (convalescent donors). Thus, we obtained peripheral blood mononuclear cells (PBMCs) from 20 donors who had cleared an asymptomatic or mild SARS-CoV-2 infection, and 19 SARS-CoV-2-naive control donors (for characteristics of donors, see Table S1). Naive control donors were defined as being seronegative for immunoglobulin G (IgG) and immunoglobulin A (IgA) targeting SARS-CoV-2 spike S1 as detected by ELISA (Figures S1A and S1B). The SARS-CoV-2-specific T cell responses were evaluated by stimulating PBMCs with overlapping peptide pools (15-mers, 11-amino acid [aa] overlap), encompassing the amino acid sequence of structural proteins (NCAP [Nucleocapsid], spike S1 + S2, VEMP [Envelope small membrane protein], VME1) and accessory proteins (AP3a, NS6, NS7a, NS7b, NS8, ORF9b, ORF10, Y14) of SARS-CoV-2. Cells were stimulated for 16 h to analyze the reactivity of T cells by flow cytometry using a set of markers for T cell activation and effector cytokine production (Figures 1A–1C). In all SARS-CoV-2 convalescent donors, we observed upregulation of cluster of differentiation (CD) 137 (4-1BB) and production of either interferon gamma (IFN- $\gamma$ ), tumor necrosis factor alpha (TNF- $\alpha$ ), or both cytokines (Figures 1D–1G), which is consistent with effector T cell activation following SARS-CoV-2-specific stimulation. Furthermore, we found SARS-CoV-2-specific CD4<sup>+</sup> and CD8<sup>+</sup> T cells responded to different viral antigens. CD4<sup>+</sup> T cells predominantly reacted to NCAP, spike S1 and S2, and to a lesser extent to VME1 (Figures 1D and 1E). In contrast, CD8<sup>+</sup> T cells predominantly reacted to NCAP, as illustrated in Figures 1F and 1G. Healthy SARS-CoV-2-seronegative control donors presented few IFN- $\gamma$ -positive CD4<sup>+</sup> T cells, whereas TNF- $\alpha$  producers responded to all tested antigens (Figures S1C and S1D). SARS-CoV-2-reactive T cells were undetectable in the CD8<sup>+</sup> T cell fraction of the seronegative control donors (Figures S1E and S1F).

#### Vector-free CRISPR/Cas9-based *FKBP12* KO in SARS-CoV-2-specific TCPs generated from convalescent donors

We have previously described a vector-free protocol for electroporation and ribonucleoprotein (RNP)-based knockout (KO) of *FKBP12* to generate Tac-resistant antiviral TCPs, which was now applied to generate SARS-CoV-2-specific Tac-resistant TCPs from eight convalescent donors (CD 1–3, 15, 17–20; Table S1).<sup>63</sup> We isolated SARS-CoV-2-specific T cells with a high purity from PBMCs, based on their IFN- $\gamma$  secretion after stimulation with SARS-CoV-2 peptide pools (NCAP, spike S1 + S2, VEMP, VME1, AP3a, NS6, NS7a, NS7b, NS8, ORF9b; ORF10, Y14) (Figures 2A–2C). These SARS-CoV-2-specific T cells were expanded and split on day 7. One-half of the culture was subsequently electroporated with RNP complexes of Cas9 and a single guide RNA (sgRNA), whereas the other half served as the unmodified control (Figure 2A). The unmodified and *FKBP12* KO SARS-CoV-2-specific T cells were expanded for a further 2 weeks (Figure 2A). Expansion rates and cell yields were similar for both fractions at days 14 and 21, illustrated in Figures 3A and 3D. Similarly, the expansion rates and total counts of CD4<sup>+</sup> and CD8<sup>+</sup> T cells of the TCPs at day 21 were comparable between unmodified and *FKBP12*<sup>KO</sup> fractions (Figures 3B and 3E). Although on day 0 we found the

CD4<sup>+</sup>/CD8<sup>+</sup> ratios were high among the SARS-CoV-2-reactive T cells, these gradually became more balanced during expansion in both unmodified and *FKBP12* KO TCPs (Figure 3F). On day 21, the KO efficiency of *FKBP12* ranged from 63% to 89% in the SARS-CoV-2-specific TCPs, as assessed by peak-shift analysis after Sanger sequencing (Figure 3C).

#### Expanded SARS-CoV-2-specific CD4<sup>+</sup> and CD8<sup>+</sup> TCPs recognize multiple SARS-CoV-2-derived antigens

Subsequently, we sought to identify the antigenic targets driving the expansion of SARS-CoV-2-specific T cells and compared their antigen specificities before and after expansion. We addressed this by re-stimulating the TCPs from both cultured unmodified controls and *FKBP12* KO with individual peptide pools of the different structural and accessory proteins of SARS-CoV-2 for 16 h.

*Ex vivo* (day 0) and post-expansion (day 21) CD4<sup>+</sup> T cells were predominantly activated by NCAP, spike S1 and S2, and VME1 (Figures 4A and 4B, S2A, S2E, and S2F). The frequency of CD4<sup>+</sup> T cell reactivity toward the different SARS-CoV-2 antigens tested was similar between *FKBP12* KO and unmodified TCPs (Figures 4B and S2C–S2F). CD8<sup>+</sup> T cells exhibited a discernably different response to the antigens tested; however, the response of the *FKBP12* KO and unmodified TCPs was again similar (Figure 4C and S2B). CD8<sup>+</sup> T cells showed greater proportions of cells reactive to NCAP and spike S1 *ex vivo* (day 0); however, after expansion (day 21), CD8<sup>+</sup> T cells responded principally to NCAP and AP3a peptide pools, whereas spike S1- and S2-specific T cells were detected at much lower frequencies than NCAP- and AP3a-specific T cells (Figures 4D, S2G, and S2H). After expansion, AP3a-specific CD8<sup>+</sup> T cells were more abundant in both unmodified and *FKBP12* KO TCPs (Figures 4D, S2C, S2D, S2G, and S2H). Interestingly, no specific activation of CD4<sup>+</sup> or CD8<sup>+</sup> T cells was observed in response to any of the other accessory proteins NS6, NS7a, NS7b, NS8, ORF9b, ORF10, and Y14 or the structural VEMP protein in both unmodified and *FKBP12* KO TCPs (Figures 4B, 4D, and S2E–S2H).

#### SARS-CoV-2-specific T cells expanded from convalescent donors display a differentiated memory phenotype

We next evaluated the cell surface expression of T cell differentiation markers of expanded unmodified control and *FKBP12* KO TCPs *ex vivo* (day 0) and after culture (day 21) (Figures 4E and 4F). In brief, the order of frequency in descending order, illustrated in Figures 4E and 4G, was observed to be: high CCR7<sup>+</sup>/CD45RA<sup>+</sup> naive T cells (T<sub>NAIVE</sub>), CCR7<sup>+</sup>/CD45RA<sup>−</sup> central memory T cells (T<sub>CM</sub>), CCR7<sup>−</sup>/CD45RA<sup>−</sup> effector memory T cells (T<sub>EM</sub>), CCR7<sup>+</sup>/CD45RA<sup>+</sup>/CD95<sup>dim</sup> stem cell-like memory T cells (T<sub>SCM</sub>), and CCR7<sup>−</sup>/CD45RA<sup>+</sup> terminally differentiated effector memory T cells (T<sub>EMRA</sub>) (Figures 4E and 4G). Post enrichment, the SARS-CoV-2-specific CD4<sup>+</sup> T cells contained a high percentage of T<sub>CM</sub> and T<sub>EM</sub> (Figures 4E and 4G). On day 21 SARS-CoV-2-specific CD4<sup>+</sup> T cells exhibited a more differentiated phenotype, with the majority being T<sub>EM</sub> in both bulk and CD137<sup>+</sup> and IFN- $\gamma$ <sup>+</sup> T cells and a lack of T<sub>CM</sub> (Figures 4F and 4H). Before enrichment, CD8<sup>+</sup> T cells presented

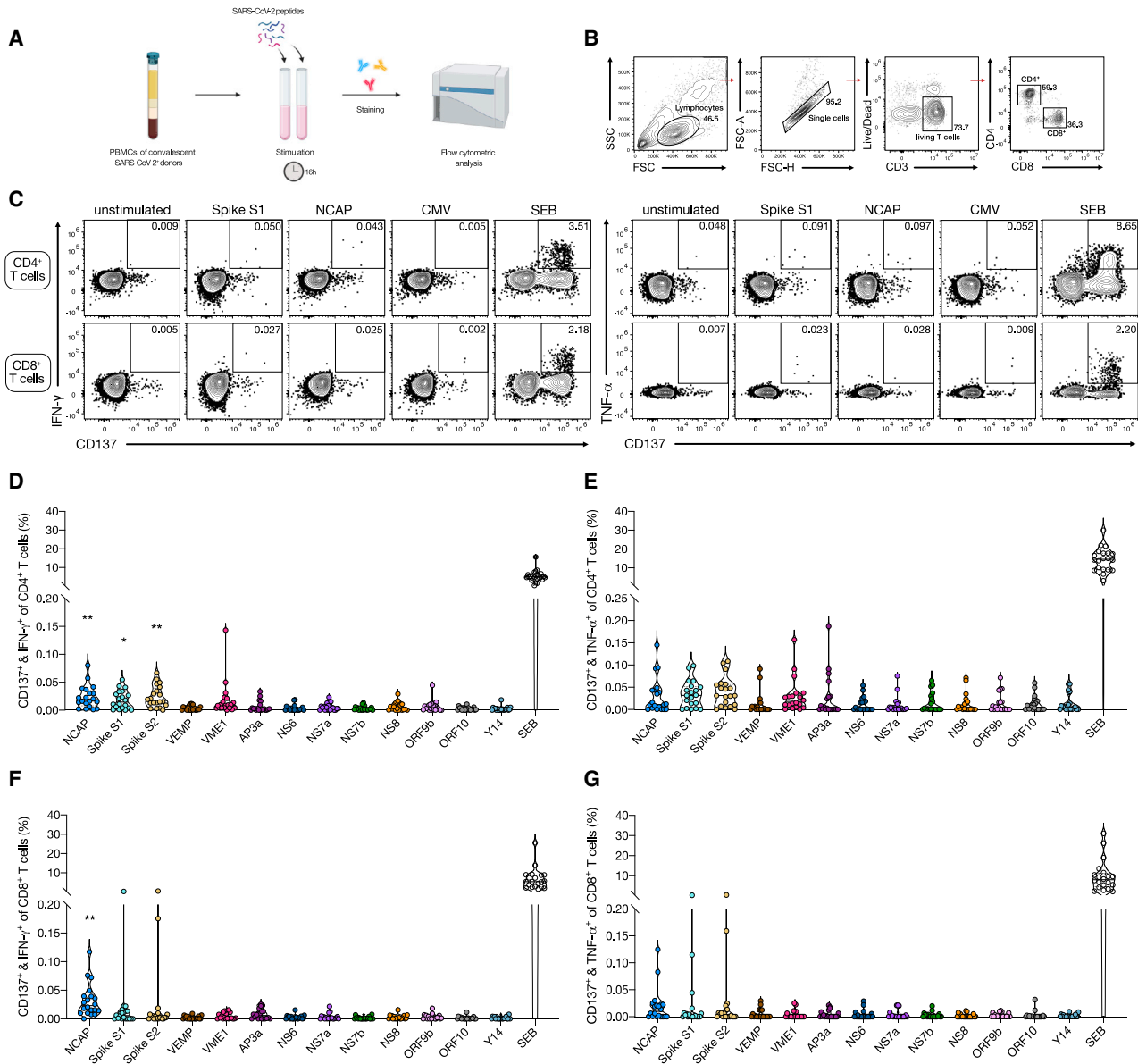


**Figure 1. Frequencies of SARS-CoV-2-reactive T cells in blood of convalescent SARS-CoV-2+ donors**

SARS-CoV-2-specific stimulation of PBMCs of convalescent SARS-CoV-2+ donors with individual structural and accessory proteins of SARS-CoV-2.  $n = 20$ ; \* $p < 0.05$ , \*\* $p < 0.01$  (statistics refer to data of seronegative healthy donors in Figures S1C–S1F). Staphylococcal enterotoxin B (SEB) serves as positive control. (A) Schematic outline of the experimental setup. Created with BioRender.com. (B) Representative gating strategy to select lymphocytes, single cells, and living CD4+ and CD8+ T cells. (C) Representative gating strategy to select antigen-reactive (CD137+) cytokine producers (IFN- $\gamma$ + or TNF- $\alpha$ +) among CD4+ and CD8+ T cells. (D) IFN- $\gamma$  production of SARS-CoV-2-activated (CD137+) CD4+ T cells after 16 h of stimulation with individual peptides of SARS-CoV-2 in convalescent SARS-CoV-2+ donors. (E) TNF- $\alpha$  production of SARS-CoV-2-activated (CD137+) CD4+ T cells after 16 h of stimulation with individual peptides of SARS-CoV-2 in convalescent SARS-CoV-2+ donors. (F) IFN- $\gamma$  production of SARS-CoV-2-activated (CD137+) CD8+ T cells after 16 h of stimulation with individual peptides of SARS-CoV-2 in convalescent SARS-CoV-2+ donors. (G) TNF- $\alpha$  production of SARS-CoV-2-activated (CD137+) CD8+ T cells after 16 h of stimulation with individual peptides of SARS-CoV-2 in convalescent SARS-CoV-2+ donors.

with an overall high frequency of  $T_{NAIVE}$ , followed by  $T_{EMRA}$  and  $T_{EM}$ , whereas  $T_{CM}$  as well as  $T_{SCM}$  were present at lower frequencies (Figures 4E and 4G). After SARS-CoV-2-specific enrichment, the CD8+ T cells contained a high proportion of  $T_{EMRA}$  and  $T_{EM}$ . On day 21 of expansion, SARS-CoV-2-specific CD8+ T cells expressed

a similar phenotype, with the majority being  $T_{EMRA}$  and  $T_{EM}$  in both bulk and CD137+ and IFN- $\gamma$ + T cells (Figures 4F and 4H). Overall, the *FKBP12* KO did not have a major effect on T cell differentiation and the subset composition of the TCPs, nor did it confer a discernible advantage to any particular subset.

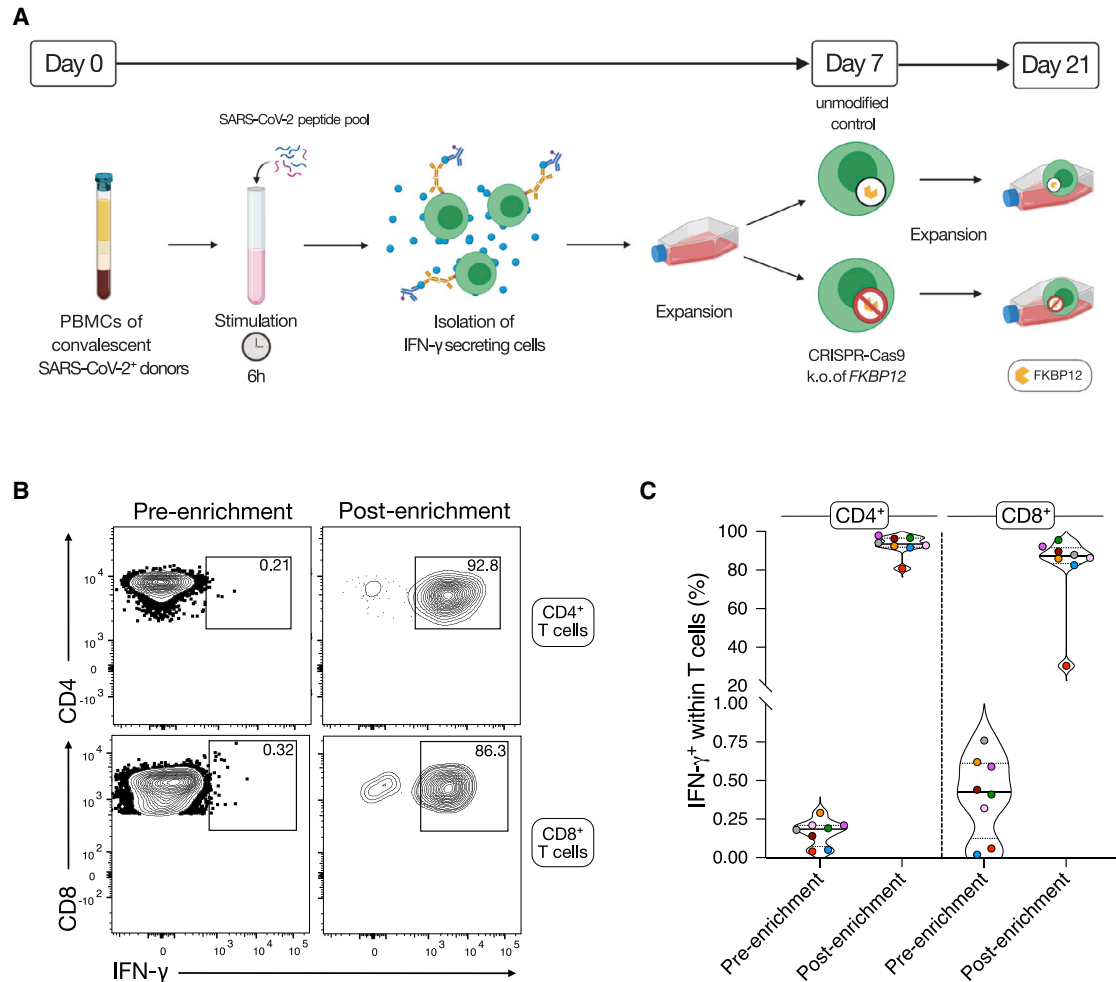


**Figure 2. Schematic outline of the experimental setup to isolate and expand SARS-CoV-2-specific T cells following CRISPR-Cas9-mediated KO of *FKBP12* to induce tacrolimus-resistance**

(A) Timeline and individual steps of the procedure to isolate and expand SARS-CoV-2-specific T cells following CRISPR-Cas9-mediated KO of *FKBP12* to induce tacrolimus-resistance. Created with [BioRender.com](https://www.biorender.com). (B) Representative dot plot of purities of SARS-CoV-2-specific IFN- $\gamma$ -producing CD4<sup>+</sup> and CD8<sup>+</sup> T cells pre and post enrichment. (C) Purities of SARS-CoV-2-specific IFN- $\gamma$ -producing CD4<sup>+</sup> and CD8<sup>+</sup> T cells pre and post enrichment, where each dot color represents one individual donor ( $n = 8$ ).

### Effector cytokine production in the presence of tacrolimus is rescued by *FKBP12* KO in SARS-CoV-2-specific TCPs

To demonstrate both efficacy against SARS-CoV-2 and to confirm Tac resistance of our *FKBP12* KO TCPs, we re-stimulated the distinct TCPs with SARS-CoV-2 peptide pools and analyzed production of antiviral cytokines (IFN- $\gamma$ , TNF- $\alpha$ , and interleukin [IL]-2) in the presence or absence of clinical doses of immunosuppressive drugs. To confirm the specificity of the *FKBP12* KO approach, we re-stimulated unmodified control and *FKBP12* KO TCPs in presence of Tac as well as an alternative CNI, CsA, which depends on the adaptor protein, peptidylprolyl isomerase A (PPIA). Thus, *FKBP12* KO should not affect the immunosuppressive function of CsA in edited TCPs. We also tested the functionality of SARS-CoV-2-specific T cells in the unmodified and *FKBP12* KO TCPs by exposure to triple immunosuppression (IS)

therapy commonly administered post solid organ transplantation, namely, Tac, prednisolone (corticosteroid), and mycophenolic acid (MPA). Upon SARS-CoV-2-specific re-stimulation on day 21, unmodified control and *FKBP12* KO TCPs showed comparable frequencies of activated (CD137<sup>+</sup>) cytokine producers among CD4<sup>+</sup> and CD8<sup>+</sup> T cells (Figures 5A–5G and S3A–S3F). Exposing TCPs to immunosuppressive drugs during stimulation resulted in a significant decrease in activated cytokine producers among CD4<sup>+</sup> (Figures 5A–5D and S3A–S3C) and CD8<sup>+</sup> T cells (Figures 5A, 5E–5G, and S3D–S3F). These were partially rescued by the *FKBP12* KO (Figures 5A–5G and S3A–S3F). Both CD4<sup>+</sup> and CD8<sup>+</sup> *FKBP12* KO T cells produced effector cytokines in the presence of Tac but not in the presence of CsA (Figures 5A–5G and S3A–S3F). The proportions of cytokine producers among CD4<sup>+</sup> and CD8<sup>+</sup> T cells in *FKBP12* KO TCPs were similar in Tac-treated

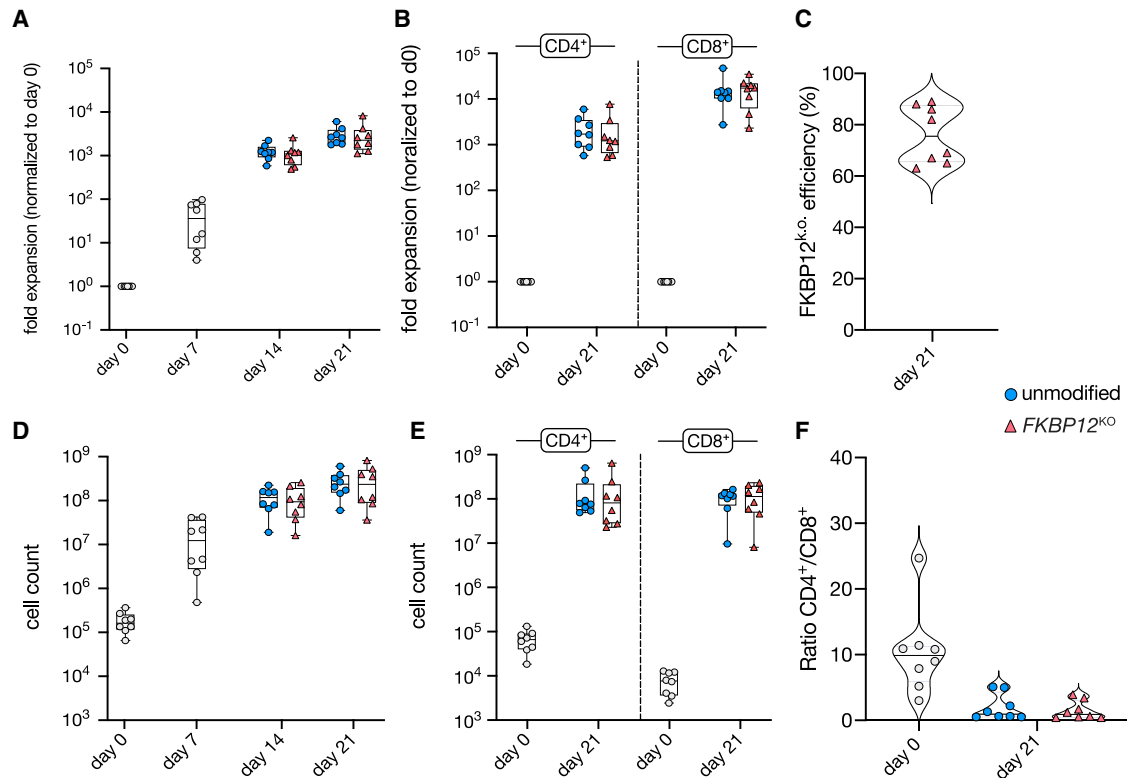


**Figure 3. Expansion rates and CD4<sup>+</sup>/CD8<sup>+</sup> T cell ratio of unmodified control and *FKBP12* KO SARS-CoV-2-specific TCPs over 21 days of culture**

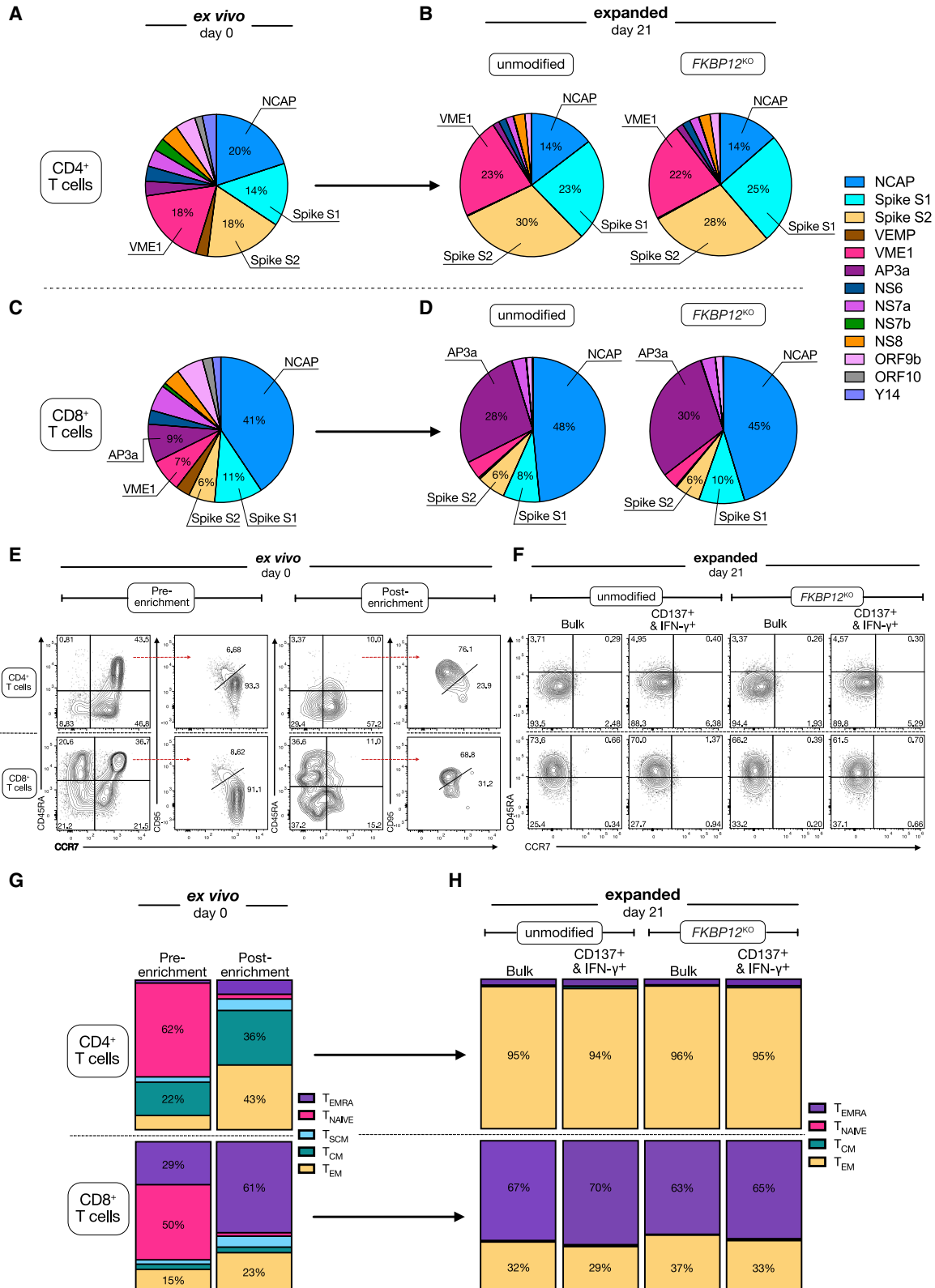
Experimental setup same as in Figure 2.  $n = 8$ . (A) Expansion rates (fold expansion) from day 0 to day 21 of unmodified control and *FKBP12* KO SARS-CoV-2-specific TCPs normalized to day 0. (B) Expansion rates (fold expansion) from day 0 to day 21 of CD4<sup>+</sup> and CD8<sup>+</sup> T cells of unmodified control and *FKBP12* KO SARS-CoV-2-specific TCPs normalized to day 0. (C) KO efficiency of *FKBP12* KO SARS-CoV-2-specific TCPs at day 21. (D) Expansion (cell count) from day 0 to day 21 of unmodified control and *FKBP12* KO SARS-CoV-2-specific TCPs. (E) Expansion (cell count) from day 0 to day 21 of CD4<sup>+</sup> and CD8<sup>+</sup> T cells of unmodified control and *FKBP12* KO SARS-CoV-2-specific TCPs. (F) Ratio of CD4<sup>+</sup>/CD8<sup>+</sup> T cells at day 0 and day 21 of unmodified control and *FKBP12* KO SARS-CoV-2-specific TCPs.

and untreated TCPs. Exposure to triple IS during stimulation decreased the capacity to produce effector cytokines among both the SARS-CoV-2-stimulated CD4<sup>+</sup> and CD8<sup>+</sup> *FKBP12* KO T cells (Figures 5A–5G and S3A–S3F). Among the CD4<sup>+</sup> and CD8<sup>+</sup> T cells of unmodified control and *FKBP12* KO TCPs, we identified polyfunctional T cells based on their ability to secrete multiple cytokines, including IFN- $\gamma$ , TNF- $\alpha$ , and IL-2 (Figures 5D, 5G, S3B, S3C, S3E, and S3F). Unlike CD4<sup>+</sup> T cells, the frequency of activated SARS-CoV-2-specific CD8<sup>+</sup> T cells, identified by CD137 (4-1BB) expression, did not significantly decrease when TCPs were exposed to CsA during stimulation (Figures S3G and S3H). However, both CD4<sup>+</sup> and CD8<sup>+</sup> CD137-expressing T cells were unable to produce effector cytokines in the presence of CsA, both in unmodified and *FKBP12* KO TCPs (Figures 5A–5G and S3A–S3F). Expression of the activation marker CD154 (CD40L) among both the SARS-CoV-2-stimulated CD4<sup>+</sup> and CD8<sup>+</sup> unmodified and *FKBP12* KO T cells was comparable. Exposing TCPs to IS during stimulation resulted in a significant decrease in CD154 expression among CD4<sup>+</sup> (Figure S3I) and CD8<sup>+</sup> T cells (Figure S3J), which was partially rescued by *FKBP12* KO.

### ***FKBP12* KO SARS-CoV-2-specific TCPs demonstrate killing capacity comparable with unmodified control SARS-CoV-2-specific TCPs**

Since targeted elimination of virus-infected cells is an essential characteristic of antiviral T cells, we tested the cytotoxic killing capacity of SARS-CoV-2-specific TCPs. Although short-term incubation with the IS Tac showed a strong effect on antiviral cytokine production in TCPs (Figure 5), we found that the T cell-mediated cytotoxic killing of target cells loaded with SARS-CoV-2 peptides was not affected by short-term treatment with Tac, neither in unmodified nor in *FKBP12* KO TCPs (Figures 6A–6C).

To identify the dominant antigens driving T cell-mediated killing of SARS-CoV-2 peptide-loaded target cells, we analyzed the killing capacity of TCPs with regard to individual antigens of SARS-CoV-2. Both unmodified control and *FKBP12* KO TCPs showed efficient killing of NCAP as well as AP3a peptide-loaded target cells, followed by target cells loaded with VME1 and spike S1 and S2 peptides (Figure 6D). We also found T cell-mediated killing toward target cells loaded with peptides from the accessory proteins NS7a and ORE9b



(legend on next page)

for some of the TCPs, but not toward target cells loaded with peptides from the remaining accessory proteins NS6, NS7b, NS8, ORF10, and Y14 or the structural protein VEMP (Figure 6D). This was in contrast to antiviral cytokine production, which we did not observe in response to accessory-protein-derived peptides in the expanded unmodified control and *FKBP12* KO TCPs, with the exception of the AP3a peptide pool (Figures 4B, 4D, and S2D–S2H). We then examined the killing capacity of CD4<sup>+</sup> and CD8<sup>+</sup> T cells separately to determine whether T cell-mediated cytotoxic killing of the dominant target antigens is executed by CD4<sup>+</sup> or CD8<sup>+</sup> T cells. Our observations suggested CD8<sup>+</sup> T cells were the main drivers of cytotoxic elimination of SARS-CoV-2 peptide-loaded target cells (Figures 6E and 6F). Among CD8<sup>+</sup> T cells of unmodified control and *FKBP12* KO TCPs, we detected the most efficient killing of NCAP, AP3a, and SARS-CoV-2 peptide-pool-loaded target cells, followed by target cells loaded with VME1, spike S1, and spike S2 peptide pools (Figures 6E and 6F).

To add another model of SARS-CoV-2 infection and to determine if the SARS-CoV-2-specific TCPs can recognize and kill these cells, we co-transfected target cells with a plasmid encoding the full sequence of the SARS-CoV-2 wild-type (WT) spike protein (pSpike) (Figure S4A) and a plasmid encoding GFP (pmaxGFP by Lonza). We sorted for GFP<sup>+</sup> target cells and co-cultured them with the distinct SARS-CoV-2-specific TCPs to determine the T cell-mediated cytotoxicity. Expression of spike was confirmed by flow cytometry (Figure S4B). We observed T cell-mediated killing of pSpike-transfected target cells by unmodified and *FKBP12* KO TCPs. Although the cytotoxic killing of SARS-CoV-2 peptide-loaded target cells by our TCPs was not affected by short-term incubation with the IS Tac (Figure 6C), we found that cytotoxic elimination of target cells transfected with pSpike was reduced in presence of Tac for unmodified but not *FKBP12* KO TCPs (Figure 6G).

#### SARS-CoV-2-specific unmodified and *FKBP12* KO TCPs recognize spike S1 and S2 of SARS-CoV-2 variants but show little cross-reactivity to spike S1 and S2 proteins of common endemic HCoVs

Considering the ongoing occurrence of SARS-CoV-2 variants, it becomes increasingly important that TCPs also recognize antigens of

the mutant SARS-CoV-2 strains without the need to determine the exact variant. Therefore, we re-stimulated the TCPs with peptide pools of the distinct spike proteins S1 and S2 of SARS-CoV-2 variants Alpha (B.1.1.7), Beta (B.1.351), Delta (B.1.617.2), and Omicron (B.1.1.529) and analyzed production of antiviral cytokines (IFN- $\gamma$  and TNF- $\alpha$ ). Upon re-stimulation with peptide pools of the spike protein S1 and S2 of SARS-CoV-2 variants, frequencies of activated (CD137<sup>+</sup>) cytokine producers among CD4<sup>+</sup> and CD8<sup>+</sup> T cells of unmodified control and *FKBP12* KO TCPs were comparable with those elicited by the WT spike S1 and S2 (Figures S5A–S5H).

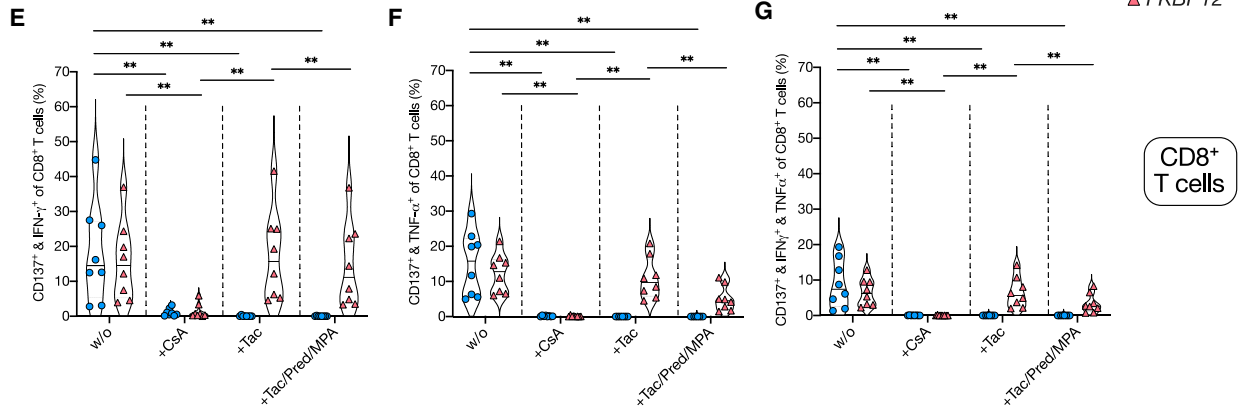
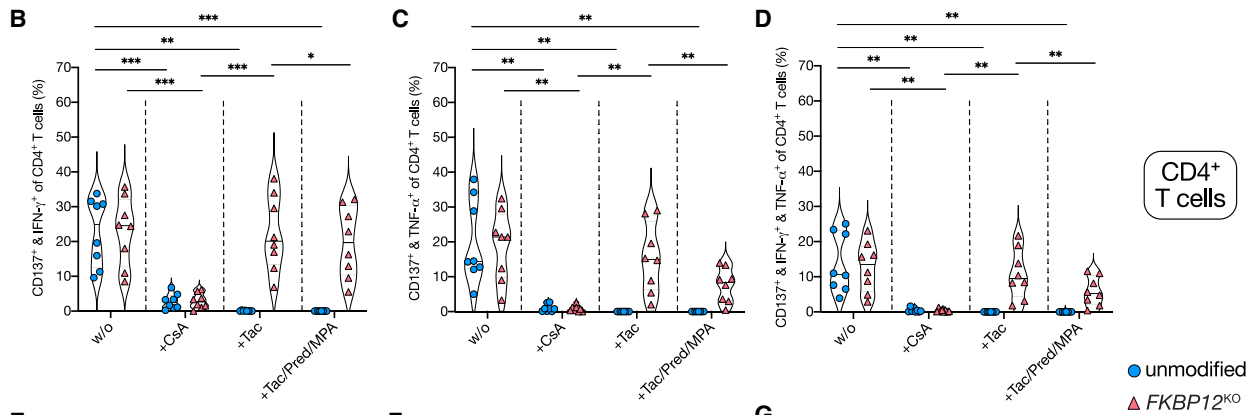
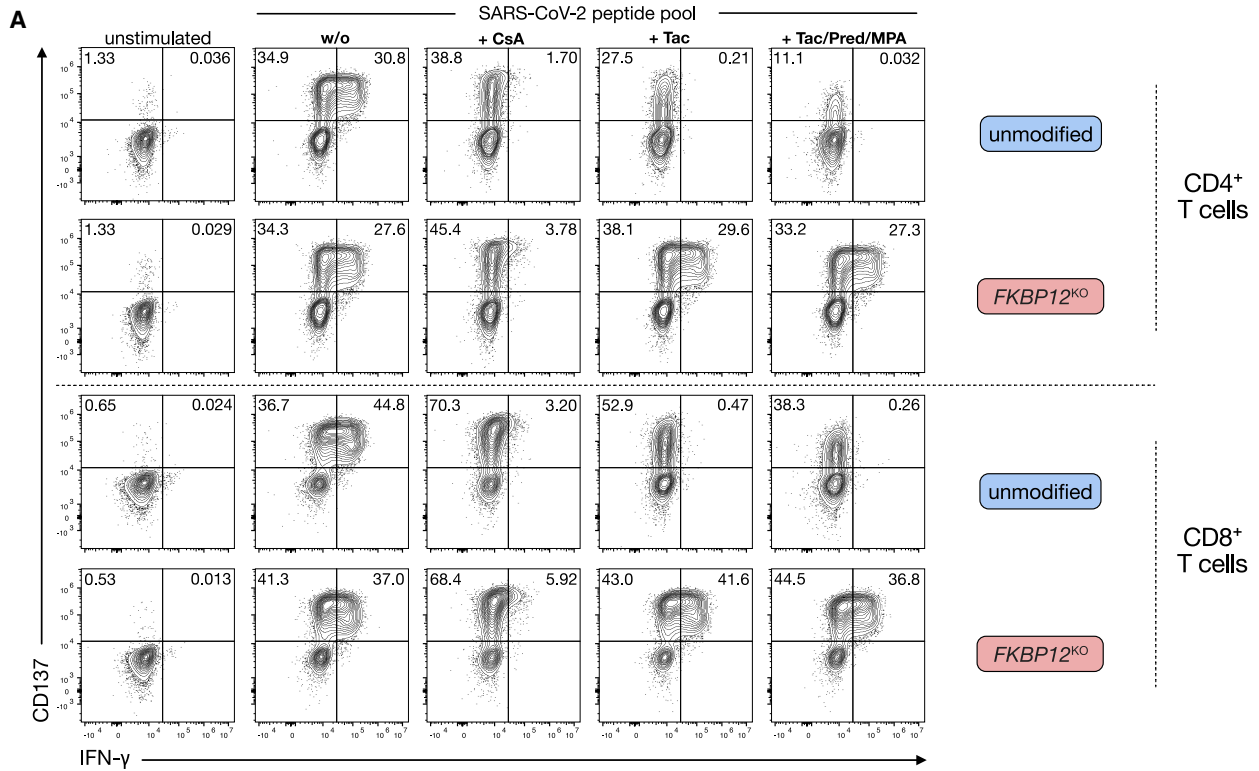
Numerous studies have suggested SARS-CoV-2 cross-reactive T cells in non-exposed individuals directed against the S2 subunit of the spike protein occur due to its partial sequence homology with common endemic HCoVs.<sup>24,25,65,66</sup> We investigated this notion by re-stimulating unmodified control and *FKBP12* KO TCPs with a peptide pool derived from spike S1 and S2 of HCoV-229E, HCoV-NL63, HCoV-OC43, and HKU1. We found that unmodified control and *FKBP12* KO TCPs showed little cross-reactivity toward spike S1 and S2 peptide pools of the common endemic HCoV (Figures S6A–S6D). For CD4<sup>+</sup> T cells, both spike S1 and S2 peptide pools of SARS-CoV-2 induced significantly higher frequencies of activated IFN- $\gamma$  as well as TNF- $\alpha$  producers in unmodified control and *FKBP12* KO TCPs compared with spike S1 and S2 peptide pools of common endemic HCoV (Figures S6A and S6B). Among the CD8<sup>+</sup> T cells, the spike S2 peptide pool of SARS-CoV-2 induced significantly higher frequencies of activated IFN- $\gamma$  as well as TNF- $\alpha$  producers in unmodified control and *FKBP12* KO TCPs compared with spike S1 and S2 peptide pools of common endemic HCoV (Figures S6C and S6D).

#### Cellular indexing of transcriptomes and epitopes sequencing and proteome analyses confirm resistance of *FKBP12* KO TCPs to tacrolimus

To determine whether *FKBP12* editing affects the transcriptome and specific surface protein levels and how these are influenced by different CNIs, we performed single-cell Cellular Indexing of Transcriptomes and Epitopes sequencing (CITE-seq) on unmodified control and *FKBP12* KO TCPs of CD17 to CD20 (Table S1). SARS-CoV-2-specific unmodified control and *FKBP12* KO TCPs

#### Figure 4. Antigen-specific T cell distribution before and after expansion of unmodified control and *FKBP12* KO SARS-CoV-2-specific TCPs

Experimental setup to define antigen specificity the same as in Figure 1, selection and expansion the same as in Figure 2. n = 8. (A) Proportional distribution of IFN- $\gamma$ -producing SARS-CoV-2-reactive (CD137<sup>+</sup>) CD4<sup>+</sup> T cells from convalescent SARS-CoV-2<sup>+</sup> donors *ex vivo* on day 0 after 16 h of stimulation with the individual structural and accessory proteins of SARS-CoV-2. (B) Proportional distribution of IFN- $\gamma$ -producing SARS-CoV-2-reactive (CD137<sup>+</sup>) CD4<sup>+</sup> T cells of unmodified control (left pie chart) and *FKBP12* KO TCPs (right pie chart) on day 21 of expansion after 16 h of stimulation with the individual structural and accessory proteins of SARS-CoV-2. (C) Proportional distribution of IFN- $\gamma$ -producing SARS-CoV-2-reactive (CD137<sup>+</sup>) CD8<sup>+</sup> T cells from convalescent SARS-CoV-2<sup>+</sup> donors *ex vivo* on day 0 after 16 h of stimulation with the individual structural and accessory proteins of SARS-CoV-2. (D) Proportional distribution of IFN- $\gamma$ -producing SARS-CoV-2-reactive (CD137<sup>+</sup>) CD8<sup>+</sup> T cells of unmodified control (left pie chart) and *FKBP12* KO TCPs (right pie chart) on day 21 of expansion after 16 h of stimulation with the individual structural and accessory proteins of SARS-CoV-2. (E) Representative flow cytometric dot plots illustrating T cell memory subsets of CD4<sup>+</sup> and CD8<sup>+</sup> T cells pre and post enrichment. (F) Representative flow cytometric dot plots illustrating T cell memory subsets of either bulk or CD137<sup>+</sup> and IFN- $\gamma$ <sup>+</sup> CD4<sup>+</sup> and CD8<sup>+</sup> T cells of unmodified control and *FKBP12* KO SARS-CoV-2-specific TCPs after 21 days of expansion. (G) Proportional distribution of T cell memory subsets of CD4<sup>+</sup> and CD8<sup>+</sup> T cells pre and post enrichment. T<sub>Naive</sub>, naive T cells (CCR7<sup>+</sup>/CD45RA<sup>+</sup>/CD95<sup>-</sup>); T<sub>SCM</sub>, stem-cell-like memory T cells (CCR7<sup>+</sup>/CD45RA<sup>+</sup>/CD95<sup>+</sup>); T<sub>CM</sub>, central memory T cells (CCR7<sup>+</sup>/CD45RA<sup>-</sup>); T<sub>EM</sub>, effector memory T cells (CCR7<sup>-</sup>/CD45RA<sup>-</sup>); T<sub>EMRA</sub>, terminally differentiated effector memory T cells (CCR7<sup>-</sup>/CD45RA<sup>+</sup>). (H) Proportional distribution of T cell memory subsets of either bulk or CD137<sup>+</sup> and IFN- $\gamma$ <sup>+</sup> CD4<sup>+</sup> and CD8<sup>+</sup> T cells of unmodified control and *FKBP12* KO SARS-CoV-2-specific TCPs after 21 days of expansion. T<sub>Naive</sub>, naive T cells (CCR7<sup>+</sup>/CD45RA<sup>+</sup>); T<sub>CM</sub>, central memory T cells (CCR7<sup>+</sup>/CD45RA<sup>-</sup>); T<sub>EM</sub>, effector memory T cells (CCR7<sup>-</sup>/CD45RA<sup>-</sup>); T<sub>EMRA</sub>, terminally differentiated effector memory T cells (CCR7<sup>-</sup>/CD45RA<sup>+</sup>).



(legend on next page)

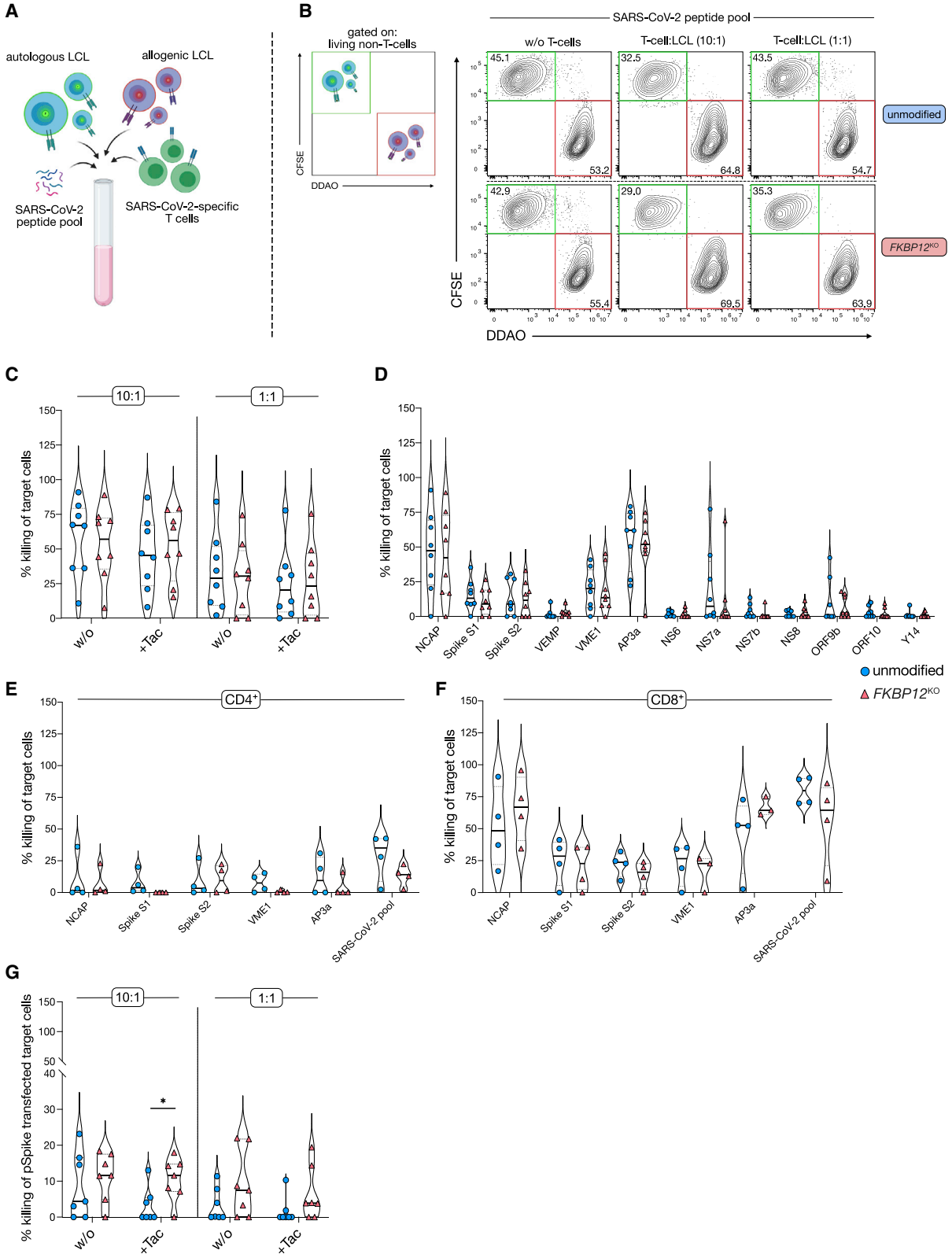
were re-stimulated with SARS-CoV-2 peptide-pool-loaded target cells for 6 h on day 21, either in the presence or absence of CNIs. According to their transcriptomes and specific protein expression identified by CITE-seq, cells were clustered by Uniform Manifold Approximation and Projection for Dimension Reduction (UMAP [Uniform manifold approximation and projection]). Twenty distinct cell clusters were identified, comprising CD4<sup>+</sup> T cells (clusters 15, 12, 2, 9, and 6), CD8<sup>+</sup> T cells (clusters 13, 17, 11, 19, 1, 5, 18, 14, and 7), double-negative (DN) T cells (cluster 16), double-positive (DP) T cells (clusters 4b, 4a, and 3), natural killer (NK) cells (clusters 20 and 10), and lymphoblastoid cell lines (LCLs) (cluster 8) (Figure 7A). RNA transcripts of genes associated with effector function (e.g., *IFNG*, *IL2*, *TNFA*, and *GZMB*) were upregulated in clusters 13 and 15 upon SARS-CoV-2-specific activation of unmodified and *FKBP12* KO TCPs (Figure 7B). However, cluster 15 but not 13 showed upregulation of *PD-1* (*PDCD1*) as well as *IL-4* mRNA. Cluster 13 additionally showed strong expression of *XCL1*, *XCL2*, *CD226*, and *IRF8*, transcripts associated with migration, survival, and memory formation,<sup>67–69</sup> which was less pronounced for cluster 15. Among both CD4<sup>+</sup> and CD8<sup>+</sup> T cells, CNI treatment as well as *FKBP12* KO had no impact on the cluster distribution in unstimulated TCPs. In contrast, upon SARS-CoV-2-specific re-stimulation, the frequency of CD4<sup>+</sup> T cell cluster 15 and CD8<sup>+</sup> T cell clusters 13 and 17 of both unmodified control and *FKBP12* KO TCPs increased. The increased frequencies of CD4<sup>+</sup> T cell cluster 15 and CD8<sup>+</sup> T cell clusters 13 and 17 were inhibited upon treatment with Tac in the unmodified control but not in *FKBP12* KO TCPs (Figure 7C). However, in the presence of CsA, CD4<sup>+</sup> T cell cluster 15 and CD8<sup>+</sup> T cell cluster 13 were under-represented in both unmodified control and *FKBP12* KO TCPs, whereas the proportion of cells falling into CD4<sup>+</sup> T cell cluster 2 and CD8<sup>+</sup> T cell clusters 17 as well as 18 increased, respectively (Figure 7C). Interestingly, cluster 2 was characterized by upregulation of *CXC3CR1* and *IL7R* mRNA, whereas cluster 17 overexpressed *ID2*, *ID3*, and *HAVCR2* (coding for TIM-3) mRNA and cluster 18 showed slightly elevated levels of *CD247* mRNA, respectively (Figure 7B). Gene expression analysis confirmed downregulation of *FKBP12* mRNA in CD4<sup>+</sup> and CD8<sup>+</sup> T cells of *FKBP12* KO TCPs (Figures S7A and S7B). Gene expression analysis also showed

that, upon SARS-CoV-2-specific stimulation, the top 25 differentially expressed genes were similar between unmodified and *FKBP12* KO TCPs in the absence of CNIs as well as under Tac treatment in the *FKBP12* KO TCPs. This was the case for both CD4<sup>+</sup> and CD8<sup>+</sup> T cell populations (Figures S7A and S7B). Remarkably, the presence of Tac further upregulated *SLA* mRNA in CD4<sup>+</sup> and *IL2* mRNA in CD8<sup>+</sup> *FKBP12*<sup>KO</sup> T cells respectively, compared with untreated *FKBP12* KO and unmodified controls. To characterize the functional capacity of *FKBP12* KO TCPs in more detail, we performed gene expression analysis of markers associated with antiviral T cell function as well as T cell exhaustion. Upon SARS-CoV-2-specific re-stimulation, CD4<sup>+</sup> T cells of unmodified and *FKBP12* KO TCPs show increased expression of *TOX2*, *EOMES*, *PDCD1*, *CTLA4*, *IL-10*, and *LAG3*, which are common markers to define T cell exhaustion (Figure S7C). When *FKBP12* KO TCPs were exposed to Tac, expression of *TOX2*, *CTLA4*, and *IL-10* was lower compared with *FKBP12* KO TCPs without Tac. CD8<sup>+</sup> T cells of unmodified and *FKBP12* KO TCPs showed increased expression of *PDCD1*, *CTLA4*, *LAG3*, and *IL10*, while the expression of *TOX2* and *EOMES* was only upregulated in unmodified but not *FKBP12* KO TCPs (Figure S7D). Moreover, CD4<sup>+</sup> and CD8<sup>+</sup> T cells of unmodified and *FKBP12* KO TCPs showed increased expression of common markers defining antiviral T cell function, including *CD40LG*, *IL21*, *IFNG*, *TNF*, *IL2*, *PRF1*, and *GZMB* in the absence of CNIs as well as under Tac treatment (Figures S7C and S7D).

To further characterize the proteomes of SARS-CoV-2-specific TCPs, we performed proteome analysis based on mass spectrometry. We confirmed the gene KO of *FKBP12* on protein level (Figure 7D). Furthermore, we detected 11 of the differentially expressed mRNA transcripts (Figures S7A and S7B) in the proteome (Figure 7D). Among those, we observed increased expression of *DDX21*, *NAMPT*, *NCL*, *PGAM1*, and *PPA1* in SARS-CoV-2-activated unmodified but not *FKBP12* KO TCPs (Figure 7D). In SARS-CoV-2-activated *FKBP12* KO TCPs, we found upregulated protein expression of *RAB27A* under Tac treatment (Figure 7D). High levels of *GZMB* were detected in *FKBP12* KO TCPs in the presence and absence of Tac, which was to a lesser extent also observed in SARS-CoV-2-activated unmodified TCPs in the absence of IS (Figure 7D).

#### Figure 5. Functional analysis of SARS-CoV-2-specific unmodified control and *FKBP12* KO TCPs

SARS-CoV-2-specific stimulation of unmodified control and *FKBP12* KO TCPs on day 21 of culture. Immunosuppressants were added where indicated: CsA, cyclosporine A; Tac, tacrolimus; Tac/Pred/MPA, tacrolimus + prednisolone + mycophenolic acid. n = 8; \*p < 0.05, \*\*p < 0.01, \*\*\*p < 0.001. (A) Representative flow cytometry plots of antigen-reactive (CD137<sup>+</sup>) IFN- $\gamma$  producers among CD4<sup>+</sup> and CD8<sup>+</sup> T cells in unmodified and *FKBP12* KO SARS-CoV-2-specific TCPs. IFN- $\gamma$  production upon SARS-CoV-2-specific re-stimulation of TCPs is shown in the presence or absence of the indicated immunosuppressants. (B) Quantified data for the IFN- $\gamma$  production of SARS-CoV-2-activated (CD137<sup>+</sup>) CD4<sup>+</sup> T cells in unmodified and *FKBP12* KO SARS-CoV-2-specific TCPs after 16 h of stimulation with SARS-CoV-2 peptide pool in the presence or absence of respective immunosuppressants. (C) Quantified data for the TNF- $\alpha$  production of SARS-CoV-2-activated (CD137<sup>+</sup>) CD4<sup>+</sup> T cells in unmodified and *FKBP12* KO SARS-CoV-2-specific TCPs after 16 h of stimulation with SARS-CoV-2 peptide pool in the presence or absence of respective immunosuppressants. (D) Quantified data for the IFN- $\gamma$  and TNF- $\alpha$  production of SARS-CoV-2-activated (CD137<sup>+</sup>) CD4<sup>+</sup> T cells in unmodified and *FKBP12* KO SARS-CoV-2-specific TCPs after 16 h of stimulation with SARS-CoV-2 peptide pool in the presence or absence of respective immunosuppressants. (E) Quantified data for the IFN- $\gamma$  production of SARS-CoV-2-activated (CD137<sup>+</sup>) CD8<sup>+</sup> T cells in unmodified and *FKBP12* KO SARS-CoV-2-specific TCPs after 16 h of stimulation with SARS-CoV-2 peptide pool in the presence or absence of respective immunosuppressants. (F) Quantified data for the TNF- $\alpha$  production of SARS-CoV-2-activated (CD137<sup>+</sup>) CD8<sup>+</sup> T cells in unmodified and *FKBP12* KO SARS-CoV-2-specific TCPs after 16 h of stimulation with SARS-CoV-2 peptide pool in the presence or absence of respective immunosuppressants. (G) Quantified data for the IFN- $\gamma$  and TNF- $\alpha$  production of SARS-CoV-2-activated (CD137<sup>+</sup>) CD8<sup>+</sup> T cells in unmodified and *FKBP12* KO SARS-CoV-2-specific TCPs after 16 h of stimulation with SARS-CoV-2 peptide pool in the presence or absence of respective immunosuppressants.



(legend on next page)

We additionally performed T cell receptor (TCR) repertoire analysis on the single-cell level to determine the effect of *FKBP12* editing on TCR diversity. Comparing the TCR clonality and total number of clones included in SARS-CoV-2-specific unmodified control and *FKBP12* KO TCPs revealed higher variations within largely expanded but low variations within single small and medium expanded clone types (Figure 7E). Importantly, there was no overrepresentation of largely expanded TCR clones within the *FKBP12* KO TCPs (Figure 7E). The TCR diversity represented by Shannon entropy was largely comparable between unmodified control and *FKBP12* KO TCPs (Figure 7F). The five most represented TCR clones within both CD4<sup>+</sup> and CD8<sup>+</sup> T cells of unmodified control and *FKBP12* KO TCPs, respectively, revealed a shared TCR repertoire with overall comparable representation of TCR clones between unmodified and *FKBP12* KO TCPs of one donor (Figure S8A). The proportion of all TCR sequences represented by the top five clones ranged from around 5% to a maximum of 32% but was comparable between *FKBP12* KO and the corresponding unmodified TCPs (Figure S8B).

## DISCUSSION

ACT is an attractive treatment strategy to prevent and treat viral infections in immunocompromised or immunosuppressed patients<sup>30–32</sup> and has been suggested as an early treatment strategy for SARS-CoV-2 infection<sup>27</sup> or even to treat acute COVID-19.<sup>28,29</sup> Immunosuppressants likely suppress endogenous antiviral immunity and could undermine the benefits of antiviral ACT, especially in patients under constant immunosuppressive treatment, such as SOT recipients.<sup>70</sup> Here, we demonstrate the feasibility of generating Tac-resistant SARS-CoV-2-specific TCPs from the blood of donors who have cleared SARS-CoV-2 infection. Tac-resistant SARS-CoV-2-specific TCPs show superior cytokine production when exposed to therapeutic doses of Tac or triple IS compared with unmodified TCPs. Tac-resistant SARS-CoV-2-specific TCPs could be used for the prevention or acute treatment of COVID-19 and enhancement of active vaccination in immunosuppressed patients on Tac therapy (transplant recipients and autoimmune patients) as well as for patients with severe COVID-19, in combination with Tac, to prevent immunopathology while achieving viral control.<sup>63</sup>

Upon SARS-CoV-2-specific stimulation of *ex vivo* PBMCs from SARS-CoV-2 convalescent donors, we detected antigen-specific CD4<sup>+</sup> and CD8<sup>+</sup> T cells, which are a pre-requisite for manufacturing

of Tac-resistant TCPs. In line with recent studies,<sup>24–26,65,66,71</sup> we found that SARS-CoV-2-specific CD4<sup>+</sup> T cells predominantly target the structural proteins NCAP, spike S1 and S2, and to a lower extent VME1, whereas CD8<sup>+</sup> T cells predominantly show specificity toward NCAP during characterization of the starting material. Similar to our observations of T cells stimulated *ex vivo* on day 0, expanded CD4<sup>+</sup> and CD8<sup>+</sup> T cells preferentially targeted different antigens of SARS-CoV-2 yet with a clear overall preference of both CD4<sup>+</sup> and CD8<sup>+</sup> T cells for the structural proteins, in line with previous reports.<sup>27,29</sup> The distribution of specificities among T cells before and after SARS-CoV-2-specific T cell expansion was largely comparable for CD4<sup>+</sup> and CD8<sup>+</sup> T cells, except for AP3a, which was found to be a relevant driver of CD8<sup>+</sup> T cell expansion and was not affected by KO of *FKBP12*. Supporting previous reports, expanded SARS-CoV-2-specific CD4<sup>+</sup> T cells recognized a broader set of viral surface antigens,<sup>27,29</sup> whereas antigen specificity for CD8<sup>+</sup> T cells was limited to internal NCAP<sup>29</sup> and AP3a.<sup>72</sup> The differences in antigen specificity between SARS-CoV-2-specific CD4<sup>+</sup> and CD8<sup>+</sup> T cells may relate to distinct processing and presentation of viral surface and internal antigens. However, it is also reported that apoptosis and autophagy are upregulated in PBMCs of SARS-CoV-2-infected individuals,<sup>73</sup> which may promote presentation of phagocytosed antigens via major histocompatibility complex (MHC) class II molecules on professional antigen-presenting cells. In line with our observations, the VEMP protein is reported to be barely recognized by the host's adaptive immune defense.<sup>74</sup> A recent report suggests that ORF8 protein downregulates the expression of MHC class I molecules on several cell types, resulting in impaired antigen presentation to CD8<sup>+</sup> T cells.<sup>75</sup> While CD8<sup>+</sup> T cells are indispensable for elimination of infected cells, CD4<sup>+</sup> T cells contribute to affinity-matured and protective antibody responses, and thus Tac-resistant TCPs may help to establish improved antibody responses in immunosuppressed individuals. Indeed, it was shown that spike-specific CD4<sup>+</sup> T cell responses correlate with serum levels of anti-spike IgG titers in recovered SARS-CoV-2-infected donors.<sup>76</sup> Moreover, VME1-specific antibodies have been suggested as an additional target for immune monitoring due to the relatively high frequency of VME1-specific CD4<sup>+</sup> T cells in the blood of convalescent COVID-19 patients.<sup>26</sup>

With the continued emergence of SARS-CoV-2 variants, we were interested in whether the SARS-CoV-2-specific TCPs we generated are cross-reactive to mutant SARS-CoV-2 strains abolishing the need for

### Figure 6. Killing capacity of SARS-CoV-2 peptide-loaded autologous target cells by unmodified control and *FKBP12* KO SARS-CoV-2-specific TCPs

SARS-CoV-2-specific T cell-mediated cytotoxicity of unmodified control and *FKBP12* KO TCPs at day 21 of culture. Immunosuppressant Tac was added where indicated. n = 8 for (C) and (D); n = 4 for (E) and (F) (except for VME1 and AP3a of *FKBP12* KO TCPs: n = 3); n = 7 for (G) \*p < 0.05. (A) Schematic illustration of the experimental setup. Created with BioRender.com. (B) Representative flow cytometry plots illustrating the selection of autologous (CFSE-labeled) and allogenic (DDAO [7-hydroxy-9H-(1,3-dichloro-9,9-dimethylacridin-2-one)]-labeled) LCLs in the different conditions indicated above the plots. (C) Percentage killing of SARS-CoV-2 peptide-pool-loaded autologous target T cells by unmodified control and *FKBP12* KO SARS-CoV-2-specific TCPs at 10:1 and 1:1 ratios (T cells:LCLs) in the presence or absence of Tac. (D) Percentage killing of autologous target cells loaded with indicated structural and accessory proteins of SARS-CoV-2 by unmodified control and *FKBP12* KO SARS-CoV-2-specific TCPs at 10:1 ratio (T cells:LCLs). (E) Percentage killing of autologous target cells loaded with indicated structural (NCAP, spike S1, spike S2, VME1, SARS-CoV-2-pool) and accessory proteins (AP3a) of SARS-CoV-2 by purified CD4<sup>+</sup> T cells of unmodified control and *FKBP12* KO SARS-CoV-2-specific TCPs at 10:1 ratio (T cells:LCLs). (F) Percentage killing of autologous target cells loaded with indicated structural (NCAP, spike S1, spike S2, VME1, SARS-CoV-2-pool) and accessory proteins (AP3a) of SARS-CoV-2 by purified CD8<sup>+</sup> T cells of unmodified control and *FKBP12* KO SARS-CoV-2-specific TCPs at 10:1 ratio (T cells:LCLs). (G) Percentage killing of autologous target cells transfected with a plasmid encoding the full spike protein of SARS-CoV-2 by unmodified control and *FKBP12* KO SARS-CoV-2-specific TCPs at 10:1 and 1:1 ratio (T cells:LCLs) in the presence or absence of Tac.

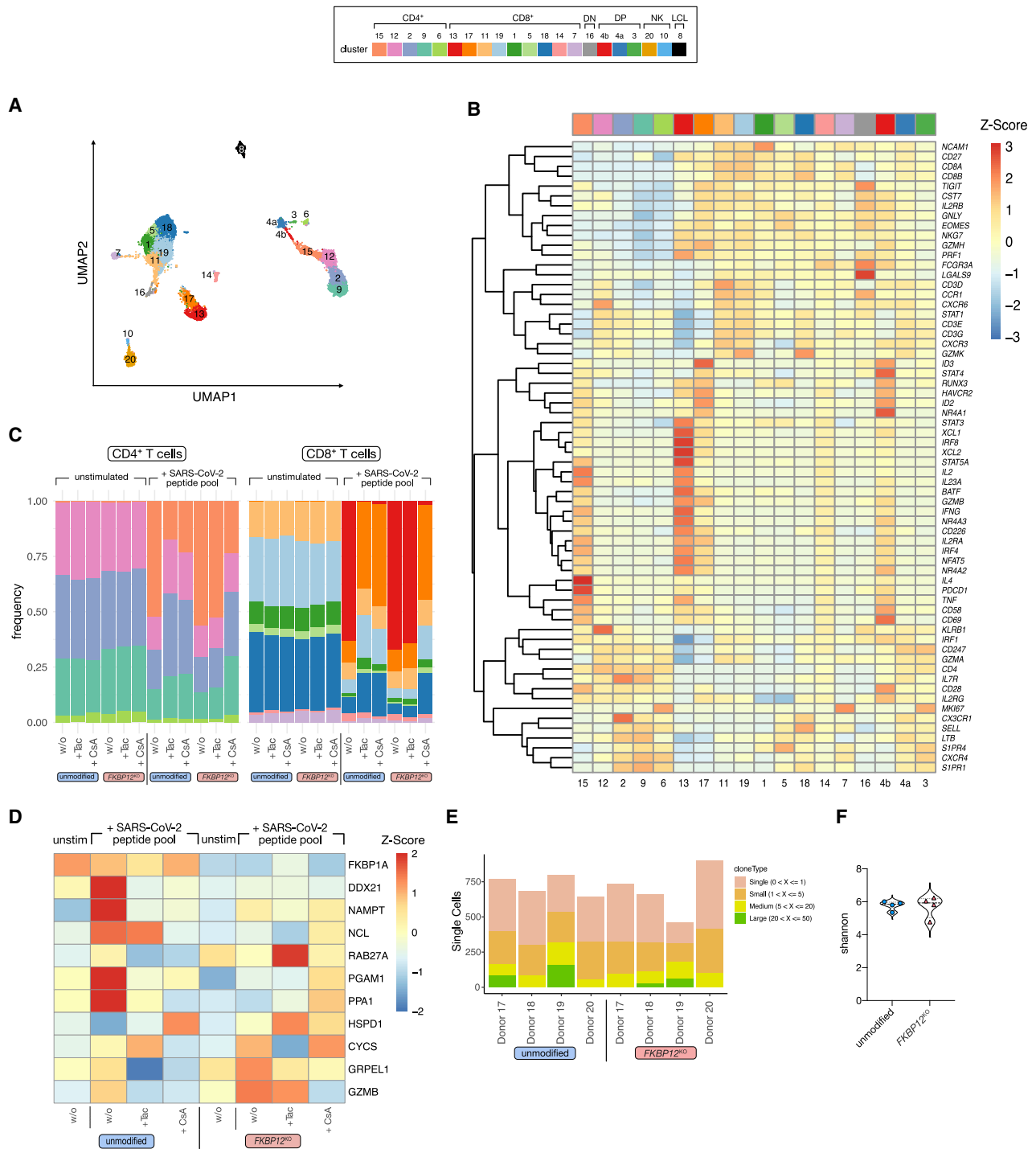


**Figure 7. Single-cell transcriptomes, proteome data, and TCR repertoire of unmodified control and FKBP12 KO SARS-CoV-2-specific TCPs**  
 CITE-seq, proteome, and TCR analysis of SARS-CoV-2-specific TCPs after SARS-CoV-2-specific re-stimulation at day 21 of culture. Immunosuppressant Tac or CsA were added where indicated. n = 4, n = 3 for (D) (A) UMAP representation of unmodified and FKBP12 KO TCPs. Transcriptionally similar clusters were identified using shared nearest neighbor (SNN) modularity optimization. (B) Heatmap of RNA expression of T cell-associated genes within different clusters. (C) Cluster distribution within unmodified control and FKBP12 KO SARS-CoV-2-specific TCPs in the presence or absence of IS as well as in unstimulated and stimulated conditions. (D) Heatmap of proteins differentially expressed upon SARS-CoV-2-specific stimulation in T cells of unmodified control and FKBP12 KO TCPs in presence or absence of IS. (E) Distribution of different clone types within unmodified control and FKBP12 KO TCPs. (F) TCR diversity represented by Shannon entropy of unmodified control and FKBP12 KO TCPs.

variant identification prior to TCP manufacturing. Both unmodified control and *FKBP12* KO TCPs recognized spike protein S1 and S2 of SARS-CoV-2 variants Alpha (B.1.1.7), Beta (B.1.351), Delta (B.1.617.2), and Omicron (B.1.1.529), and elicited effector cytokine levels similar to WT spike S1 and S2 peptide pools, which is in line with recent reports.<sup>77,78</sup> This observation confirms that the T cell response in SARS-CoV-2 convalescent or vaccinated individuals remains largely stable even against mutants of SARS-CoV-2, whereas neutralizing antibodies are reported to be weakened in their effect.<sup>77,79</sup>

Cross-reactive SARS-CoV-2 T cell epitopes with predominant spike specificity have been described in unexposed individuals, which might be due to previous infections with common endemic HCoV.<sup>80</sup> In agreement with recent studies, we observed higher frequencies of SARS-CoV-2 cross-reactive T cells among CD4<sup>+</sup> compared with CD8<sup>+</sup> T cells<sup>65,80–82</sup> in the seronegative healthy individuals from our study. There is evidence that pre-formed SARS-CoV-2-directed immunity to structural proteins is not driven by cross-reactivity to common endemic HCoV but rather by other frequently encountered pathogens.<sup>83</sup> Hence, the exact source of pre-formed T cell immunity in SARS-CoV-2-naïve individuals remains to be elucidated. To date, it remains uncertain whether cross-reactive memory T cells possess protective features to fight SARS-CoV-2 infection.<sup>84</sup> Our data from convalescent donors indicate little cross-reactivity of SARS-CoV-2-specific TCPs toward spike S1 and S2 of common endemic HCoV after expansion. In line with this, when stimulating PBMCs of convalescent SARS-CoV-2-infected donors with spike peptide pools from either SARS-CoV-2, common endemic HCoV-229E, or HCoV-OC43, it was reported that frequencies of SARS-CoV-2 spike-specific CD4<sup>+</sup> T cells were significantly higher than spike-299E- or spike-OC43-specific CD4<sup>+</sup> T cells.<sup>74</sup> This indicates that the T cell response toward spike protein is predominantly directed against SARS-CoV-2 in these donors. Although it has been reported that, after coronavirus infection, spike-specific T cells can persist for as long as 4 years,<sup>85</sup> the frequency of cross-reactive T cells in the blood might be limited since memory T cells are known to reside in the bone marrow and, without substantial viral re-stimulation, it is unlikely that they egress into the blood stream.<sup>86</sup>

Patients who experience mild symptoms following SARS-CoV-2 infection show higher proportions of CD8<sup>+</sup> T cell responses compared with those suffering from severe infection,<sup>42,76</sup> suggesting a potential protective role of CD8<sup>+</sup> T cell immunity against SARS-CoV-2. CD8<sup>+</sup> T cells are known to contribute to effective viral clearance to terminate acute viral infections, whereas cytotoxic CD4<sup>+</sup> T cells are required to control chronic infections by, e.g., human immunodeficiency virus or herpes viruses.<sup>87</sup> We found that CD8<sup>+</sup> T cells were the main drivers of SARS-CoV-2-directed cytotoxicity to SARS-CoV-2-loaded target cells. Although starting with a small proportion of SARS-CoV-2-reactive CD8<sup>+</sup> T cells on day 0, we obtained a more balanced CD8<sup>+</sup> to CD4<sup>+</sup> T cell ratio on day 21 of *in vitro* expansion. Contrary to our observations, Keller et al. (2020) did not obtain strong SARS-CoV-2-specific CD8<sup>+</sup> T cell responses using peptide libraries consisting of only SARS-CoV-2 structural proteins to isolate SARS-

CoV-2-specific T cells, neither immediately after isolation nor after expansion.<sup>27</sup> It may be that a combination of structural and accessory antigens of SARS-CoV-2 is superior in driving expansion of both CD4<sup>+</sup> and CD8<sup>+</sup> SARS-CoV-2-directed T cells.<sup>29</sup> Furthermore, the cytokine cocktail within the culture medium may affect the expansion of either CD4<sup>+</sup> or CD8<sup>+</sup> T cells.<sup>88</sup> Therefore, the use of different cytokine cocktails may explain the observed variations in the expansion of SARS-CoV-2-specific CD8<sup>+</sup> T cells.

Upon SARS-CoV-2-specific *ex vivo* stimulation, multiple studies have reported high proportions of T<sub>EMRA</sub> in the SARS-CoV-2-specific CD8<sup>+</sup> T cell compartment of patients who have recovered from SARS-CoV-2 infection.<sup>65,76,89</sup> Prior to expansion, SARS-CoV-2-specific CD8<sup>+</sup> T cells comprised a substantial proportion of T<sub>EMRA</sub>.<sup>28</sup> This highly differentiated memory phenotype might therefore be characteristic of SARS-CoV-2 infection, suggesting short-term CD8<sup>+</sup> T cell immunity. T cells with effector memory and central memory phenotypes have previously been shown to exhibit increased *in vivo* persistence after adoptive transfer and to induce long-term immunity,<sup>90</sup> and would therefore be desirable for ACT, whereas a terminally differentiated phenotype would not.<sup>91</sup> Analysis of the T cell phenotype of the *FKBP12* KO TCPs revealed a predominant T<sub>EM</sub> and T<sub>CM</sub> phenotype among CD4<sup>+</sup> T cells before and after SARS-CoV-2-induced T cell expansion, whereas CD8<sup>+</sup> T cells displayed mainly a T<sub>EMRA</sub> phenotype followed by T<sub>EM</sub> as the second most represented memory T cell subset, which was also the case for unmodified control TCPs. This may raise concerns about the efficacy, longevity, and induction of functional memory by TCPs. However, in patients suffering from severe COVID-19, parameters including longevity and memory formation of the TCPs may not necessarily be required to clear an acute SARS-CoV-2 infection. Moreover, T<sub>EMRA</sub> can be divided into several subsets that have been shown to differ in their ability to differentiate, proliferate, and produce effector cytokines<sup>92–94</sup> and might even comprise cells evolved from a naive differentiation stage.<sup>93</sup> It is conceivable that SARS-CoV-2-specific CD8<sup>+</sup> T cells with a late-differentiated effector phenotype could de-differentiate into long-lived memory cells.<sup>94</sup> Low-dose rapamycin supplementation during cell expansion may be a potential strategy to arrest differentiation of SARS-CoV-2-reactive T cells or to generate early-differentiated T cells.<sup>88,95</sup> Ultimately, clinical trials are needed to answer the question of efficacy of TCPs with high T<sub>EMRA</sub> content to fight or prevent SARS-CoV-2 infection.

Our functional analysis of the SARS-CoV-2-specific TCPs has shown that the innovative *FKBP12* KO TCPs possess superior cytokine production upon SARS-CoV-2-specific re-stimulation in the presence of Tac and triple IS compared with unmodified SARS-CoV-2-specific TCPs. The sensitivity of *FKBP12* KO SARS-CoV-2-specific TCPs toward CsA shows specificity of the approach and represents an important safety switch, which could limit undesired toxicity associated with Tac-resistant *FKBP12* KO SARS-CoV-2-specific TCPs *in vivo*.<sup>43</sup> In line with previous observations, Tac did not influence the cytotoxic killing capacity of either unmodified or *FKBP12* KO SARS-CoV-2-specific TCPs when confronted with peptide-loaded target cells.<sup>63,96</sup>

However, Tac treatment did influence T cell-mediated cytotoxic killing of pSpike-transfected target cells. The transfection of spike protein likely leads to a reduced or selective antigen presentation by target cells compared with the usage of a peptide pool. Indeed, Tac has been reported to interfere with antigen presentation.<sup>97,98</sup> Thus, the system, which requires active antigen presentation by the LCLs as opposed to the passive presentation of peptides, may be more susceptible to Tac, since a certain TCR signaling threshold is necessary to achieve full T cell activation.<sup>99</sup> Re-stimulation using a SARS-CoV-2 peptide pool may be able to continuously exceed this threshold irrespective of the presence of Tac, whereas it is not reached in the case of transfection with pSpike due to the diminished antigen presentation in the presence of Tac.

*FKBP12* KO TCPs may also support antibody production in Tac-treated patients as they show CD154 expression upon SARS-CoV-2-specific re-stimulation in the presence of Tac and triple IS, which was not the case for unmodified SARS-CoV-2-specific TCPs. We also confirmed upregulation of CD154 (CD40LG) mRNA transcripts upon SARS-CoV-2-specific re-stimulation of both unmodified and *FKBP12* KO TCPs as well as expression of IL-21 mRNA, which are both important for antigen-specific B cell development and maturation as well as the formation of long-lived plasma cells and memory B cells.<sup>100,101</sup> Virus-specific T cell polyfunctionality is a correlate of T cell efficacy and immune protection.<sup>102,103</sup> Since *FKBP12* KO SARS-CoV-2-specific TCPs contain multiple effector cytokine producers (even in the presence of Tac), our approach holds promise for adoptively inducing protective immunity against SARS-CoV-2.

Single-cell CITE-seq identified distinct cell clusters based on specific cell surface protein expression and their transcriptomes. Cluster distributions were comparable among CD4<sup>+</sup> and CD8<sup>+</sup> T cells between non-activated unmodified control and *FKBP12* KO SARS-CoV-2-specific TCPs even in the presence of Tac or CsA. Upon SARS-CoV-2-specific activation, a distinct cluster distribution was observed. For CD4<sup>+</sup> T cells, the frequency of cluster 15, and for CD8<sup>+</sup> T cells the frequency of clusters 13 and 17, increased in the absence of CNIs for unmodified and *FKBP12* KO TCPs as well as in the presence of Tac for *FKBP12* KO TCPs, which demonstrates that neither *FKBP12* editing nor Tac treatment affected the transcriptome or expression of specific proteins of the inventive *FKBP12* KO TCPs. Gene expression signatures revealed CD4<sup>+</sup> T cell cluster 15 and CD8<sup>+</sup> T cell cluster 13 represented T cells with effector functions. Upregulated expression of *PD-1* was detected for cluster 15 but not cluster 13, indicating that expanded SARS-CoV-2-specific CD4<sup>+</sup> effector T cells might be more prone to T cell exhaustion than their CD8<sup>+</sup> counterparts. Furthermore, high IL-4 expression in T cells allocated to cluster 15 points out the presence of CD4<sup>+</sup> T<sub>H2</sub> cells known to suppress IFN- $\gamma$ -producing CD4<sup>+</sup> T<sub>H1</sub> cells.<sup>104</sup> However, IL-4 is also involved in immunoglobulin class switching and therefore the development and maturation of antigen-specific B cells and the formation of long-lived plasma cells and memory B cells.<sup>101</sup> Within CD8<sup>+</sup> T cell cluster 13, we observed higher expression of *XCL1*, *XCL2*, *CD226*, and *IRF8*, which

was less pronounced for CD4<sup>+</sup> T cell cluster 15. These genes are known to be expressed by CD8<sup>+</sup> effector T cells and support cell migration as well as memory formation and cell survival.<sup>67–69</sup> Gene expression patterns confirmed downregulation of *FKBP12* mRNA in *FKBP12* KO TCPs. The top 25 differentially expressed genes among SARS-CoV-2-specific activated CD4<sup>+</sup> and CD8<sup>+</sup> T cells of unmodified control and *FKBP12* KO TCPs in the absence of CNI as well as under Tac treatment in the *FKBP12* KO TCPs comprised genes mainly associated with metabolism, zinc-finger proteins, as well as proteins of the transcriptional machinery. Interestingly, *IL-2* was higher in SARS-CoV-2-stimulated *FKBP12* KO CD8<sup>+</sup> T cells exposed to Tac compared with non-exposed *FKBP12* KO CD8<sup>+</sup> T cells and unmodified controls. IL-2-producing CD8<sup>+</sup> antiviral T cells are associated with high proliferative potential and are promising candidates to induce sustained immunity after adoptive transfer.<sup>105</sup> Moreover, upregulation of *CXC3CR1* and *IL7R* mRNA in CD4<sup>+</sup> T cell cluster 2 implies T cells with high effector function and migratory capacity.<sup>106–108</sup> For CD8<sup>+</sup> T cell cluster 17, we found overexpression of *ID2* and *ID3*, which are reported to promote survival and differentiation of mature effector CD8<sup>+</sup> T cells.<sup>109</sup> Furthermore, upregulation of *HAVCR2* mRNA in CD8<sup>+</sup> T cell cluster 17 could have beneficial effects on TCR-dependent activation and, therefore, could enhance effector functions of our TCPs.<sup>110</sup> A slight increase in *CD247* mRNA levels within CD8<sup>+</sup> T cell cluster 18 could result in reduced susceptibility to apoptosis.<sup>111</sup> Gene expression analysis of markers associated with antiviral T cell function or T cell exhaustion revealed upregulation of *TOX2*, a key player in T cell development, which regulates T cell persistence and exhaustion and is induced upon strong antigen stimulation in T cells,<sup>112</sup> and *EOMES*, an important transcription factor for memory T cells, although high levels of *EOMES* can promote T cell exhaustion.<sup>113</sup> The unmodified TCPs show higher *TOX2* and *EOMES* expression compared with *FKBP12* KO TCPs, indicating that the *FKBP12* KO TCPs tend to be less exhausted, presumably due to reduced Ca<sup>2+</sup> influx into the cytoplasm and thus reduced Ca<sup>2+</sup>-dependent activation.<sup>114</sup> We also observed upregulation of some co-inhibitory receptors among CD4<sup>+</sup> and CD8<sup>+</sup> T cells in both unmodified and *FKBP12* KO TCPs, including PD-1 (*PDCD1*), CTLA-4, LAG-3, and IL-10. However, we also detected upregulated expression of genes associated with antiviral T cell function, including IFN- $\gamma$ , TNF- $\alpha$ , IL-2, as well as perforin and granzyme B (*GZMB*). Exhausted T cells are characterized by the loss of effector cytokine production combined with high co-expression of inhibitory receptors.<sup>115</sup> Although we observed upregulation of some exhaustion markers in both of our SARS-CoV-2-specific TCPs, we also found that they retain their antiviral effector function, furthermore, many of the exhaustion markers are not exclusive to exhausted cells but are also upregulated upon activation. Thus, we conclude that our TCPs show strong antiviral function and only minor signs of T cell exhaustion. Moreover, proteome data confirmed downregulation of *FKBP12* on the protein level in *FKBP12* KO TCPs. SARS-CoV-2-activated unmodified but not *FKBP12* KO TCPs showed upregulated expression of proteins involved in RNA processing, cell metabolism, and shuttling, such

as DDX21,<sup>116</sup> NAMPT,<sup>117</sup> NCL,<sup>118</sup> PGAM1,<sup>119</sup> and PPA1.<sup>120</sup> We observed upregulated expression of RAB27A in SARS-CoV-2-specific *FKBP12* KO TCPs under Tac treatment, indicating increased lysosomal secretory capacity compared with unmodified TCPs.<sup>121</sup> We also confirmed upregulation of the antiviral T cell marker GZMB on the protein level in *FKBP12* KO TCPs in the presence and absence of Tac. On the mRNA level, we observed upregulation of all these genes in SARS-CoV-2-activated unmodified and *FKBP12* KO TCPs. The differences between mRNA and protein expression patterns might be due to post-translational stabilization or preferential degradation of certain proteins. In summary, the proteome data confirmed the observed Tac resistance of SARS-CoV-2-specific *FKBP12* KO TCPs as well as upregulation of GZMB, and further indicate superior lysosomal function compared with unmodified TCPs.

TCR diversity was largely comparable between unmodified control and *FKBP12* KO TCPs. The distribution of the top five most represented TCR clones within CD4<sup>+</sup> and CD8<sup>+</sup> T cells of unmodified control and *FKBP12* KO TCPs revealed a shared TCR repertoire with no signs of abnormal proliferation of individual clones, which would be the case if *FKBP12* KO or potential off-target editing transformed certain clones. Therefore, we conclude that our novel strategy of *FKBP12* editing neither skewed the TCR repertoire of TCPs nor induced excessive clonal expansion.

Taken together, we have demonstrated the feasibility of manufacturing GMP-compatible Tac-resistant SARS-CoV-2-specific TCPs with superior function in the presence of Tac and triple IS compared with unmodified control SARS-CoV-2-specific TCPs. The retained sensitivity to CsA represents an important safety switch to inhibit potential adverse effects elicited by *FKBP12*-edited TCPs *in vivo*. Our innovative GMP-compliant protocol to generate *FKBP12* KO SARS-CoV-2 specific TCPs qualifies for transfer into clinical application,<sup>63</sup> since we have already shown this is feasible in our previous study.<sup>88,122</sup> We are preparing for clinical translation of Tac-resistant SARS-CoV-2-specific TCPs for first-in-human use in SOT recipients or autoimmune patients on Tac therapy as a proof of concept. Transplant patients may specifically benefit from Tac-resistant ACT as their responses toward active SARS-CoV-2 vaccination are reported to be poor<sup>18,123</sup> and therefore could be improved if patients have previously undergone Tac-resistant ACT as a passive vaccination strategy. Importantly, Tac therapy combined with adoptive transfer of Tac-resistant SARS-CoV-2 TCPs may be an attractive novel treatment concept to prevent undesired immune reactions such as alloreactivity, autoimmunity, or hyperinflammation while efficiently treating viral infections such as severe COVID-19.

## MATERIALS AND METHODS

### Blood sampling and PBMC isolation

The study was approved by the Charité – Universitätsmedizin Berlin Ethics Committee and peripheral blood was obtained from convalescent individuals with a history of asymptomatic or mild COVID-19 or SARS-CoV-2 seronegative healthy donors, who had given their writ-

ten informed consent. PBMCs were isolated using Biocoll (Biochrom) gradient centrifugation.

### Determining SARS-CoV-2-specific T cell responses

PBMCs ( $2 \times 10^6$ ) were stimulated with peptide pools of individual proteins of SARS-CoV-2 (JPT Peptide Technologies; i.e., NCAP, spike S1, spike S2, VEMP, VME1, AP3a, NS6, NS7a, NS7b, NS8, ORF9b, ORF10, Y14) at 1 µg/mL each in the presence of 1 µg/mL purified anti-CD28 antibody (clone CD28.2, BioLegend). Unstimulated controls were supplemented with equal concentrations of DMSO and 4 mg/mL staphylococcal enterotoxin B (SEB) (Sigma-Aldrich), and CMV peptide pool (pp65 and IE-1; 0.5 µg/mL each; JPT Peptide Technologies) served as positive controls. Stimulated PBMCs were incubated in a humidified incubator at 37°C, 5% CO<sub>2</sub> for 16 h. Intracellular cytokine production was captured by addition of 2 µg/mL Brefeldin A (Sigma-Aldrich) after 2 h of stimulation, and cells were stained using antibodies (all from BioLegend) and the FoxP3/Transcription Factor Staining Buffer Set (eBioscience). Staining was performed using fluorophore-conjugated human anti-CD3 (OKT3), -CD4 (SK3), -CD8 (RPA-T8), -IFN-γ (4S.B3), -TNF-α (Mab11), -IL-2 (MQ1-17H12), -CD137 (4B4-1), -CD154 (24-31), -CCR7 (G043H7), and -CD45RA (HI100) antibodies. LIVE/DEAD Fixable Blue Dead Cell Stain (L/D; Invitrogen) was used to exclude dead cells. Samples were analyzed using a CytoFLEX flow cytometer (Beckman Coulter) and FlowJo-10 software (Tree Star).

### Serology

Serum IgG and IgA levels of antibodies targeting the S1 domain of the spike glycoprotein were determined by using anti-SARS-CoV-2 spike 1 IgG and IgA ELISA and carried out according to the manufacturers protocol (EUROIMMUN).

### Isolation and culture of SARS-CoV-2-specific T cells

Virus-specific T cells were isolated from PBMCs derived from 100 mL of peripheral blood from convalescent donors following a 6-h stimulation with overlapping SARS-CoV-2-specific peptide pools (JPT Peptide Technologies; 1 µg/mL each) using an IFN-γ Secretion Assay—Cell Enrichment and Detection Kit according to the manufacturer's instructions (Miltenyi Biotec). Isolated virus-specific T cells were cultured in complete medium (VLE RPMI 1640 [PAN-Biotech] supplemented with penicillin [100 IU/mL], streptomycin [Biochrom], 10% fetal calf serum [FCS, PAA], 10 ng/mL recombinant human IL-7 [rhIL-7] and rhIL-15 [CellGenix]) in 24-well plates, in humidified incubators at 37°C and 5% CO<sub>2</sub> as described previously.<sup>88,122</sup> Cells were split 1:1 upon reaching 100% confluency.

### KO procedure

Two million to 10 million antiviral T cells (half of the culture derived from 100 mL of peripheral blood) were electroporated with RNPs on day 7 of expansion using Amaxa P3 primary cell 4D-Nucleofector X Kit L and the Amaxa-Nucleofector-4D (Lonza, program CO-115) to transfer ribonucleoprotein complexes of 30 µg of recombinant Alt-R Sp. HiFi Cas9 Nuclease V3 (Integrated DNA Technologies)<sup>124</sup>

precomplexed with 15 µg of synthetically modified sgRNA targeting 5'-GGGCGCACCTTCCCCAAGCG-3' with 2O'-methyl-3'-phosphothioate modifications between the first and last three nucleotides (Synthego Corporation). The same number of unmodified antiviral T cells were expanded as controls.

#### Phenotypic and functional assays assessed by flow cytometry

For assessing SARS-CoV-2-specific cytokine production/activation, LCLs were generated as described previously<sup>125</sup> and used as antigen-presenting cells at a 1:10 ratio for a 16-h SARS-CoV-2-specific stimulation with 0.65 µg/mL of pooled SARS-CoV-2-specific peptides (JPT Peptide Technologies) in the presence or absence of immunosuppressants at clinical doses (6 ng/mL tacrolimus [Prograf, Astellas]; 120 ng/mL CsA [Sandimmun, Novartis]; triple IS = 6 ng/mL tacrolimus + 0.57 µg/mL prednisolone [Urbason soluble, Sanofi] + 2.7 µg/mL MPA [active substance of mycophenolate mofetil; Sigma-Aldrich]). Additionally, T cells were re-stimulated using peptide pools of individual SARS-CoV-2 proteins (NCAP, spike S1, spike S2, VEMP, VME1, AP3a, NS6, NS7a, NS7b, NS8, ORF9b, ORF10, Y14) (JPT Peptide Technologies; 0.5 µg/mL). To determine cross-reactivity to SARS-CoV-2 variants, cryopreserved TCPs were thawed and re-stimulated with a pool of peptides spanning the sequences of spike proteins of Alpha (B.1.1.7), Beta (B.1.351), Delta (B.1.617.2), and Omicron (B.1.1.529) (JPT Peptide Technologies; 0.5 µg/mL). To assess potential cross-reactivity to other common HCoV, TCPs were re-stimulated with a pool of peptides spanning the sequences of spike proteins of common endemic HCOVs (HCoV-229E, HCoV-NL63, HCoV-OC43, HKU1) (JPT Peptide Technologies; 0.5 µg/mL). Re-stimulation with CEFX Ultra Superstim pool (JPT Peptide Technologies; 0.5 µg/mL) served as control to exclude nonspecific T cell expansion. Unstimulated controls included LCLs without SARS-CoV-2-specific peptides. Intracellular cytokine production was captured by addition of 2 µg/mL of Brefeldin A (Sigma-Aldrich) after 2 h of stimulation and cells were stained using antibodies (all from BioLegend, unless stated otherwise) and the FoxP3/Transcription Factor Staining Buffer Set (eBioscience). Staining was performed using fluorophore-conjugated human anti-CD3 (OKT3), -CD4 (SK3), -CD8 (RPA-T8), -IFN-γ (4S.B3), -TNF-α (MAb11), -IL-2 (MQ1-17H12), -CD137 (4B4-1), -CD154 (24-31), -CCR7 (G043H7), and -CD45RA (HI100) antibodies. LIVE/DEAD Fixable Blue Dead Cell Stain (L/D; Invitrogen) was used to exclude dead cells.

A VITAL assay was performed to assess the killing capacity of TCPs.<sup>88,126,127</sup> Briefly, cells from TCPs were incubated at distinct ratios with autologous LCLs loaded with SARS-CoV-2-peptide pool or with peptide pools of individual SARS-CoV-2 proteins and stained with 10 µM carboxyfluorescein diacetate succinimidyl ester (CFSE-DA; Sigma-Aldrich) for 4 min, whereas unloaded allogenic LCLs serving as non-target controls were stained with 5 µM CellTrace Far Red (Invitrogen) for 10 min. T cell-free LCL mixtures served as internal controls to calculate the SARS-CoV-2-specific killing capacity. After 14 h of incubation, co-cultures were stained with L/D.

To assess the killing capacity of SARS-CoV-2 spike protein-transfected target cells by TCPs, we performed another VITAL assay. From  $8 \times 10^6$  to  $10 \times 10^6$  autologous LCLs were co-transfected with 4 µg of plasmid encoding SARS-CoV-2 spike protein (pSpike) and 4 µg of pmaxGFP (Lonza) via electroporation using Amaxa P3 primary cell 4D-Nucleofector X Kit L and the Amaxa-Nucleofector-4D (Lonza, program DS-104). After 24 h, GFP<sup>+</sup> LCLs were sorted at the Sony Sorter MA900. Spike expression of sorted GFP<sup>+</sup> target cells was confirmed by flow cytometry using an anti-spike-RBD AF647 antibody (Invitrogen). Cryopreserved TCPs were thawed and incubated at distinct ratios with GFP<sup>+</sup>/pSpike-transfected LCLs, whereas unloaded allogenic LCLs serving as non-target control were stained with 5 µM CellTrace Far Red (Invitrogen) for 10 min. T cell-free LCL mixtures served as internal controls to calculate the SARS-CoV-2-specific killing capacity. After 14 h of incubation, co-cultures were stained with L/D.

The SARS-CoV-2-specific killing capacity was calculated according to the following formulas:

$$\text{Ratio T - cell - free LCL mixtures: } \frac{\% \text{ target cells}}{\% \text{ non - target cells}}$$

$$\% \text{ killing of target cells} = 100$$

$$- \frac{\frac{\% \text{ target cells}}{\% \text{ non - target cells}}}{\text{Ratio T - cell - free LCL mixtures}} * 100$$

All flow cytometry samples were analyzed using either a CytoFLEX or Navios flow cytometer (both Beckman Coulter) and FlowJo-10 software (Tree Star).

#### KO efficiency analysis

Analysis of on-target gene editing was performed on isolated DNA (Zymo Research) from day 21 cell samples. The *FKBP12* locus was amplified using KAPA HiFi HotStart ReadyMix (Roche) and the following primer pairs: TCTGACGGGTCAGATAACACCTAG (F) and TCTTCCGGAGGCCTGGGTTT (R) with the following touch-down-PCR program in an automated thermocycler: (1) 95°C, 3 min; (2) 98°C, 30 s; (3) 72°C to 64°C, 15 s (−0.5°C for each cycle starting at the highest until the lowest temperature was reached; 20 cycles, 64°C); (4) 72°C, 15 s; (5) repeat from step (2) with decreasing annealing temperature (as specified); (6) 72°C, 1 min; (7) 4°C. PCR products were purified using DNA purification and enrichment kit (Zymo Research) prior to Sanger sequencing with primer F by LGC Genomics. Editing frequencies were calculated using the Inference of CRISPR Edits (ICE) algorithm (Synthego Corporation).

#### Proteomics

Cryopreserved *in vitro* expanded SARS-CoV-2-specific unmodified and *FKBP12* KO T cells were thawed and re-stimulated with SARS-CoV-2 peptide pool-loaded LCLs for 6 h and subsequently T cells were purified with the Sony sorter MA900 and cell pellets were frozen in liquid nitrogen and stored at −80°C. Further sample preparation

and analysis via nano-liquid chromatography-tandem mass spectrometry was performed as already described elsewhere.<sup>128</sup> The acquired raw files were analyzed by data analysis (Version 3.0, Bruker Daltonic, Bremen, Germany). The derived peak lists were searched against the human Swiss-Prot database using PEAKS studio proteomics software version 7.5 (Bioinformatics Solutions, Waterloo, Canada). Default settings were used with PEAKS studio proteomics software version 7.5 without merging the scans. Correct precursor was detected using mass only. Peptide identifications were performed within PEAKS using its own search engine PEAKS DB combined with PEAKS *de novo* sequencing. PEAKS PTM search tool was used to search for unspecified peptides that are homologous to peptides in the protein database. The default maximum number of variable post-translational modifications per peptide was three. Retention time shift tolerance was 1 min. All the search tools are included in the PEAKS studio software. False discovery rate (FDR) was estimated with target decoy fusion and set to 0.01. Label-free quantification with PEAKS Q was used. PEAKS was allowed to autodetect the reference sample and automatically align the sample runs. To allow the exporting of complete results, protein significance filter was set to 0, protein fold change filter to 1, and unique peptide filter to 1 in the export settings. They were considered just for high-confidence interaction of active interaction sources by experiments, databases, co-expression, and co-occurrences. Differentially abundant proteins were identified using ANOVA. To validate genes at the protein level, top differentially regulated genes in CD4<sup>+</sup> and CD8<sup>+</sup> T cells and a manual selection of exhaustion/activation genes were intersected with the complete list of proteins. The shortlisted proteins were then tested for interaction between *FKBP12* KO and tacrolimus-treatment in LCL-stimulated T cells.

### Single-cell CITE-seq and TCR sequencing

*In vitro* expanded SARS-CoV-2-specific unmodified and *FKBP12* KO T cells were labelled with anti-human TotalSeq-C hashtag antibodies (BioLegend) allowing the pooling of samples followed by labelling with anti-human TotalSeq-C antibodies (BioLegend) targeting a selection of extracellular proteins (Table S2).<sup>129</sup> Single-cell suspensions were loaded onto Next GEM Chip G (10X Genomics), which were placed into a 10X Genomics controller for initiation of the 10X workflow. Transcriptome, antibody-derived, and TCR libraries were prepared using the Chromium Single Cell 5' Library and Gel Bead Kit as well as the Single Cell 5' Feature Barcode Library Kit (10X Genomics). TCR targeting was performed using the Chromium Single Cell V(D)J Enrichment Kit for Human T cells (10X Genomics). Gene expression and TCR libraries were prepared using the Single Index Kit T Set A, whereas the Single Index Kit N Set A (10X Genomics) was used for antibody-derived libraries.

Qubit HS DNA assay kit (Life Technologies) was used for library quantification, and fragment sizes were obtained using the 2100 Bioanalyzer using the High Sensitivity DNA Kit (Agilent). Sequencing was performed on a NextSeq500 device (Illumina) using High Output v2 Kits (150 cycles) with the recommended sequencing conditions for 5' GEX libraries (read1, 26 nt; read2, 98 nt; index1, 8 nt; index2, not

available [n.a.]) and Mid Output v2 Kits (300 cycles) for TCR/BCR libraries (read1, 150 nt, read2, 150 nt, index1, 8 nt, index2, n.a., 20% PhiX spike-in).

### Single-cell CITE-seq and TCR sequencing analysis

Raw sequence reads were processed using Cell Ranger 5.0.0, including the default detection of intact cells. Mkfastq and count were used in default parameter settings for demultiplexing and quantifying the gene expression. Refdata-cellranger-hg19-1.2.0 was used as reference. Raw UMI (Unique Molecular Identifier) counts were further processed and analyzed using R 4.0.2 according to the osca workflow by Lun et al.,<sup>130</sup> including normalization, filtering of low-quality cells, clustering, and UMAP dimensionality reduction. Differentially abundant genes and clusters were identified using edgeR's quasi-likelihood methods and test for interaction between *FKBP12* KO and tacrolimus treatment in LCL-stimulated cells. TCR repertoire analysis was conducted on the filtered\_contig\_annotations.csv outputs from the 10X Genomics Cell Ranger pipeline using the scRepertoire package.<sup>131</sup> Clonotypes were called using the combination of CDR3 nucleotide sequences and genes.

### Statistics

p values were determined by tests for normal distribution (Shapiro-Wilk and Kolmogorov-Smirnov tests), followed by one-way ANOVA (normally distributed data sets) or Friedman test (not normally distributed data sets) and paired t tests (normally distributed data sets) or Wilcoxon matched pairs signed rank tests (not normally distributed data sets) or Mann-Whitney-U test (not normally distributed data sets) as posttests. GraphPad Prism 9 (GraphPad Software) and R (version 3.5.2) were used to generate graphs and carry out the statistical analysis of data. Graphical schemes were designed using BioRender 2022 ([www.biorender.com](http://www.biorender.com)).

### SUPPLEMENTAL INFORMATION

Supplemental information can be found online at <https://doi.org/10.1016/j.omtm.2022.02.012>.

### ACKNOWLEDGMENTS

We thank all voluntary blood donors for their donations. We thank Dr. Pawel Durek and Dr. Frederik Heinrich for processing of sequencing data. We thank Dr. Nicola R. Brindle for language editing and Dr. Jaspal Kaeda and Dr. Martin Szyska for critical revision of the manuscript. Funding: the study was generously supported in parts by the German Federal Ministry of Education and Research (BIH Center for Regenerative Therapies, 10178 Berlin – H.-D.V., P.R., L.A., M.S.-H.), two research grants by the Einstein Center for Regenerative Therapies (L.P., L.A., G.Z., M.S.-H.), the state of Berlin and the European Regional Development Fund (ERDF 2014–2020, EFRE 1.8/11, Deutsches Rheuma-Forschungszentrum) (M.-F.M.), the Berlin Institute of Health (BIH) with the Starting Grant-Multi-Omics Characterization of SARS-CoV-2 infection, Project 6, Identifying Immunological Targets in Covid-19 (M.-F.M.), a BIH Translation-Mission-Fund, a Crossfield project fund of the BIH Research Focus Regenerative Medicine (D.J.W., H.-D.V., P.R., L.A., M.S.-H.) and a BIH Research

Platform Clinical Translational Sciences grant (L.A., M.S.-H.). This work received funding by the Federal Ministry of Education and Research, “Determining and Using Immunity to SARS-CoV-2 (COVIM)” and “A Platform to Specifically Regenerate Antiviral T cell Responses Avoiding Unwanted Bystander Immune Reactions in a Novel Personalized Therapy Approach: TReAT (Tacrolimus-resistant Antiviral T-cell Therapy - 01EK2104A).” The funders had no role in study design, data collection and analysis, decision to publish, or preparation of the manuscript.

#### AUTHOR CONTRIBUTIONS

L.P. planned and performed experiments, composed the figures, analyzed results, interpreted the data, and wrote the manuscript. D.J.W., H.H., R.N., D.L.W., G.Z., S.M., S.P., and S.Schlickeiser performed experiments and revised the manuscript. S. Schlickeiser performed statistical analyses, and analyzed and interpreted the data. M.-F.M. supervised single-cell data acquisition and provided the necessary infrastructure. O.K. performed proteomics data acquisition and analysis. H.M., M.G., T.R., and N.B. developed and provided the plasmid encoding SARS-CoV-2 spike protein and supported the experimental procedure. H.-D.V. and P.R. provided infrastructure, interpreted the data, and edited the manuscript. L.A. and M.S.-H. led the project, designed the research, interpreted the data, and wrote the manuscript. All authors discussed, commented on, and approved the manuscript in its final form.

#### DECLARATION OF INTERESTS

D.L.W., H.-D.V., P.R., L.A., and M.S.-H. have a patent pending on immunosuppressant-resistant T cells for adoptive immunotherapy. All other authors declare no competing interests.

#### REFERENCES

- Du, Y., Tu, L., Zhu, P., Mu, M., Wang, R., Yang, P., Wang, X., Hu, C., Ping, R., Hu, P., et al. (2020). Clinical features of 85 fatal cases of COVID-19 from Wuhan: a retrospective observational study. *Am. J. Respir. Crit. Care Med.* *201*, 1372–1379.
- Wu, Z., and McGoogan, J.M. (2020). Characteristics of and important lessons from the coronavirus disease 2019 (COVID-19) outbreak in China: summary of a report of 72314 cases from the Chinese center for disease control and prevention. *J. Am. Med. Assoc.* *323*, 1239–1242.
- Alfishawy, M., Elbendary, A., Mohamed, M., and Nassar, M. (2020). COVID-19 mortality in transplant recipients. *Int. J. Organ Transpl. Med.* *11*, 145.
- Gianfrancesco, M., Hyrich, K.L., Hyrich, K.L., Al-Adely, S., Al-Adely, S., Carmona, L., Danila, M.I., Gossec, L., Gossec, L., Izadi, Z., et al. (2020). Characteristics associated with hospitalisation for COVID-19 in people with rheumatic disease: data from the COVID-19 Global Rheumatology Alliance physician-reported registry. *Ann. Rheum. Dis.* *79*, 859–866.
- de Candia, P., Prattichizzo, F., Garavelli, S., and Matarese, G. (2021). T cells: warriors of SARS-CoV-2 infection. *Trends Immunol.* *42*, 18–30.
- Hassan, I.A., Chopra, R., Swindell, R., and Mutton, K.J. (2003). Respiratory viral infections after bone marrow/peripheral stem-cell transplantation: the Christie hospital experience. *Bone Marrow Transpl.* *32*, 73–77.
- Manuel, O., and Estabrook, M. (2019). RNA respiratory viral infections in solid organ transplant recipients: guidelines from the American Society of Transplantation Infectious Diseases Community of Practice. *Clin. Transpl.* *33*, e13511.
- Kim, Y.-J., Boeckh, M., and Englund, J.A. (2007). Community respiratory virus infections in immunocompromised patients: hematopoietic stem cell and solid organ transplant recipients, and individuals with human immunodeficiency virus infection. *Semin. Res. Crit. Care Med.* *28*, 222–242.
- Pereira, M.R., Mohan, S., Cohen, D.J., Husain, S.A., Dube, G.K., Ratner, L.E., Arcasoy, S., Aversa, M.M., Benvenuto, L.J., Dadhania, D.M., et al. (2020). COVID-19 in solid organ transplant recipients: initial report from the US epicenter. *Am. J. Transpl.* *20*, 1800–1808.
- Kates, O.S., Haydel, B.M., Florman, S.S., Rana, M.M., Chaudhry, Z.S., Ramesh, M.S., Safa, K., Kotton, C.N., Blumberg, E.A., Besharatian, B.D., et al. (2020). Coronavirus disease 2019 in solid organ transplant: a multicenter cohort study. *Clin. Infect. Dis.* *73*, e4090–e4099.
- Alberici, F., Delbarba, E., Manenti, C., Econimo, L., Valerio, F., Pola, A., Maffei, C., Possenti, S., Zambetti, N., Moscato, M., et al. (2020). A single center observational study of the clinical characteristics and short-term outcome of 20 kidney transplant patients admitted for SARS-CoV2 pneumonia. *Kidney Int.* *97*, 1083–1088.
- Fernández-Ruiz, M., Andrés, A., Loinaz, C., Delgado, J.F., López-Medrano, F., San Juan, R., González, E., Polanco, N., Folgueira, M.D., Lalueza, A., et al. (2020). COVID-19 in solid organ transplant recipients: a single-center case series from Spain. *Am. J. Transpl.* *20*, 1849–1858.
- Requião-Moura, L.R., de Sandes-Freitas, T.V., Viana, L.A., Cristelli, M.P., de Andrade, L.G.M., Garcia, V.D., de Oliveira, C.M.C., de Esmeraldo, R.M., Filho, M.A., Pacheco-Silva, A., et al. (2021). High mortality among kidney transplant recipients diagnosed with coronavirus disease 2019: results from the Brazilian multicenter cohort study. *PLoS One* *16*, e0254822.
- Vinson, A.J., Agarwal, G., Dai, R., Anzalone, A.J., Lee, S.B., French, E., Olex, A., Madhira, V., and Mannon, R.B. (2021). COVID-19 in solid organ transplantation: results of the national COVID cohort collaborative. *Transpl. Direct* *7*, e775.
- Collier, D.A., Ferreira, I.A.T.M., Kotagiri, P., Datir, R.P., Lim, E.Y., Touizer, E., Meng, B., Abdullahi, A., Elmer, A., Kingston, N., et al. (2021). Age-related immune response heterogeneity to SARS-CoV-2 vaccine BNT162b2. *Nature* *596*, 417–422.
- Hyams, C., Marlow, R., Maseko, Z., King, J., Ward, L., Fox, K., Heath, R., Turner, A., Friedrich, Z., Morrison, L., et al. (2021). Effectiveness of BNT162b2 and ChAdOx1 nCoV-19 COVID-19 vaccination at preventing hospitalisations in people aged at least 80 years: a test-negative, case-control study. *Lancet Infect. Dis.* *21*, 1539–1548.
- Boyersky, B.J., Werbel, W.A., Avery, R.K., Tobian, A.A.R., Massie, A.B., Segev, D.L., and Garonzik-Wang, J.M. (2021). Antibody response to 2-dose sars-cov-2 mrna vaccine series in solid organ transplant recipients. *J. Am. Med. Assoc.* *325*, 2204–2206.
- Bertrand, D., Hamzaoui, M., Lemée, V., Lamulle, J., Hanoy, M., Laurent, C., Lebourg, L., Etienne, I., Lemoine, M., Le Roy, F., et al. (2021). Antibody and T Cell response to SARS-CoV-2 messenger RNA BNT162b2 vaccine in kidney transplant recipients and hemodialysis patients. *J. Am. Soc. Nephrol.* *32*, 2147–2152.
- Prendecki, M., Clarke, C., Edwards, H., McIntyre, S., Mortimer, P., Gleeson, S., Martin, P., Thomson, T., Randell, P., Shah, A., et al. (2021). Humoral and T-cell responses to SARS-CoV-2 vaccination in patients receiving immunosuppression. *Ann. Rheum. Dis.* *80*, 1322–1329.
- Stumpf, J., Siepmann, T., Lindner, T., Karger, C., Schwöbel, J., Anders, L., Faulhaber-Walter, R., Schewe, J., Martin, H., Schirutschke, H., et al. (2021). Humoral and cellular immunity to SARS-CoV-2 vaccination in renal transplant versus dialysis patients: a prospective, multicenter observational study using mRNA-1273 or BNT162b2 mRNA vaccine. *Lancet Reg. Heal. Eur.* *9*, 100178.
- Loconsole, D., Stea, E.D., Sallustio, A., Fontò, G., Pronzo, V., Simone, S., Centrone, F., Accogli, M., Gesualdo, L., and Chironna, M. (2021). Severe COVID-19 by SARS-CoV-2 lineage B.1.1.7 in vaccinated solid-organ transplant recipients: new preventive strategies needed to protect immunocompromised patients. *Vaccines* *9*, 806.
- Ali, N.M., Alnazari, N., Mehta, S.A., Boyarsky, B., Avery, R.K., Segev, D.L., Montgomery, R.A., and Stewart, Z.A. (2021). Development of COVID-19 infection in transplant recipients after SARS-CoV-2 vaccination. *Transplantation* *105*, E104–E106.
- Wadei, H.M., Gonwa, T.A., Leoni, J.C., Shah, S.Z., Aslam, N., and Speicher, L.L. (2021). COVID-19 infection in solid organ transplant recipients after SARS-CoV-2 vaccination. *Am. J. Transpl.* *21*, 3496–3499.
- Braun, J., Loyal, L., Frentsch, M., Wendisch, D., Georg, P., Kurth, F., Hippenstiel, S., Dingeldey, M., Kruse, B., Fauchere, F., et al. (2020). SARS-CoV-2-reactive T cells in healthy donors and patients with COVID-19. *Nature* *587*, 270–274.

25. Grifoni, A., Weiskopf, D., Ramirez, S.I., Mateus, J., Dan, J.M., Moderbacher, C.R., Rawlings, S.A., Sutherland, A., Premkumar, L., Jadi, R.S., et al. (2020). Targets of T Cell responses to SARS-CoV-2 coronavirus in humans with COVID-19 disease and unexposed individuals. *Cell* *181*, 1489–1501.e15.
26. Thieme, C., Anft, M., Paniskaki, K., Blázquez Navarro, A., Doevelaar, A., Seibert, F.S., Hölzer, B., Konik, M.J., Brenner, T., Tempfer, C., et al. (2020). The SARS-CoV-2 T-Cell Immunity Is Directed against the Spike, Membrane, and Nucleocapsid Protein and Associated with COVID 19 Severity (SSRN Electron).
27. Keller, M.D., Harris, K.M., Jensen-Wachspress, M.A., Kankate, V.V., Lang, H., Lazarski, C.A., Durkee-Shock, J., Lee, P.H., Chaudhry, K., Webber, K., et al. (2020). SARS-CoV-2-specific T cells are rapidly expanded for therapeutic use and target conserved regions of the membrane protein. *Blood* *136*, 2905–2917.
28. Leung, W., Soh, T.G., Linn, Y.C., Low, J.G., Loh, J., Chan, M., Chng, W.J., Koh, L.P., Poon, M.L., Ng, K.P., et al. (2020). Rapid production of clinical-grade SARS-CoV-2 specific T cells. *Adv. Cell Gene Ther.* *3*, e101.
29. Basar, R., Uprety, N., Ensley, E., Daher, M., Klein, K., Martinez, F., Aung, F., Shanley, M., Hu, B., Gokdemir, E., et al. (2021). Generation of glucocorticoid-resistant SARS-CoV-2 T cells for adoptive cell therapy. *Cell Rep.* *36*, 109432.
30. Haque, T., Wilkie, G.M., Jones, M.M., Higgins, C.D., Urquhart, G., Wingate, P., Burns, D., McAulay, K., Turner, M., Bellamy, C., et al. (2007). Allogeneic cytotoxic T-cell therapy for EBV-positive posttransplantation lymphoproliferative disease: results of a phase 2 multicenter clinical trial. *Blood* *110*, 1123–1131.
31. O'Reilly, R.J., Prockop, S., Hasan, A.N., Koehne, G., and Doubrovina, E. (2016). Virus-specific T-cell banks for “off the shelf” adoptive therapy of refractory infections. *Bone Marrow Transpl.* *51*, 1163–1172.
32. Cruz, C.R., Hanley, P.J., Liu, H., Torrano, V., Lin, Y.F., Arce, J.A., Gottschalk, S., Savello, B., Dotti, G., Louis, C.U., et al. (2010). Adverse events following infusion of T cells for adoptive immunotherapy: a 10-year experience. *Cytotherapy* *12*, 743–749.
33. Hegde, M., Joseph, S.K., Pashankar, F., DeRenzo, C., Sanber, K., Navai, S., Byrd, T.T., Hicks, J., Xu, M.L., Gerken, C., et al. (2020). Tumor response and endogenous immune reactivity after administration of HER2 CAR T cells in a child with metastatic rhabdomyosarcoma. *Nat. Commun.* *11*, 1–15.
34. Dan, J.M., Mateus, J., Kato, Y., Hastie, K.M., Yu, E.D., Faliti, C.E., Grifoni, A., Ramirez, S.I., Haupt, S., Frazier, A., et al. (2021). Immunological memory to SARS-CoV-2 assessed for up to 8 months after infection. *Science* *371*, 1–7.
35. Thieme, C.J., Abou-el-Enein, M., Fritsche, E., Anft, M., Paniskaki, K., Skrzypczyk, S., Doevelaar, A., Elsallab, M., Brindle, N., Blázquez-Navarro, A., et al. (2021). Detection of SARS-CoV-2-specific memory B cells to delineate long-term COVID-19 immunity. *Allergy Eur. J. Allergy Clin. Immunol.* *76*, 2595–2599.
36. Siddiqi, H.K., and Mehra, M.R. (2020). COVID-19 illness in native and immunosuppressed states: a clinical-therapeutic staging proposal. *J. Hear. Lung Transpl.* *39*, 405–407.
37. Vabret, N., Britton, G.J., Gruber, C., Hegde, S., Kim, J., Kuksin, M., Levantovsky, R., Malle, L., Moreira, A., Park, M.D., et al. (2020). Immunology of COVID-19: current state of the science. *Immunity* *52*, 910–941.
38. Xu, Z., Shi, L., Wang, Y., Zhang, J., Huang, L., Zhang, C., Liu, S., Zhao, P., Liu, H., Zhu, L., et al. (2020). Pathological findings of COVID-19 associated with acute respiratory distress syndrome. *Lancet Respir. Med.* *8*, 420–422.
39. Song, J.W., Zhang, C., Fan, X., Meng, F.P., Xu, Z., Xia, P., Cao, W.J., Yang, T., Dai, X.P., Wang, S.Y., et al. (2020). Immunological and inflammatory profiles in mild and severe cases of COVID-19. *Nat. Commun.* *11*, 1–10.
40. Wang, F., Hou, H., Luo, Y., Tang, G., Wu, S., Huang, M., Liu, W., Zhu, Y., Lin, Q., Mao, L., et al. (2020). The laboratory tests and host immunity of COVID-19 patients with different severity of illness. *JCI Insight* *5*, e137799.
41. Diao, B., Wang, C., Tan, Y., Chen, X., Liu, Y., Ning, L., Chen, L., Li, M., Liu, Y., Wang, G., et al. (2020). Reduction and functional exhaustion of T cells in patients with coronavirus disease 2019 (COVID-19). *Front. Immunol.* *11*, 827.
42. Zheng, M., Gao, Y., Wang, G., Song, G., Liu, S., Sun, D., Xu, Y., and Tian, Z. (2020). Functional exhaustion of antiviral lymphocytes in COVID-19 patients. *Cell Mol. Immunol.* *17*, 533–535.
43. Zhou, F., Yu, T., Du, R., Fan, G., Liu, Y., Liu, Z., Xiang, J., Wang, Y., Song, B., Gu, X., et al. (2020). Clinical course and risk factors for mortality of adult inpatients with COVID-19 in Wuhan, China: a retrospective cohort study. *Lancet* *395*, 1054–1062.
44. (2020). Dexamethasone in hospitalized patients with covid-19 preliminary report. *N. Engl. J. Med.* *NEJMoa2021436*. <https://doi.org/10.1056/2FNEJMoa2021436>.
45. Peter, H., Wei Shen, L., Jonathan R, E., Marion, M., Jennifer L, B., Louise, L., Natalie, S., Christopher, S., Andrew, U., Einas, E., et al. (2021). Dexamethasone in hospitalized patients with covid-19. *N. Engl. J. Med.* *384*, 693–704.
46. Wu, C., Chen, X., Cai, Y., Xia, J., Zhou, X., Xu, S., Huang, H., Zhang, L., Zhou, X., Du, C., et al. (2020). Risk factors associated with acute respiratory distress syndrome and death in patients with coronavirus disease 2019 pneumonia in wuhan, China. *JAMA Intern. Med.* *180*, 934.
47. Auyeung, T.W., Lee, J.S.W., Lai, W.K., Choi, C.H., Lee, H.K., Lee, J.S., Li, P.C., Lok, K.H., Ng, Y.Y., Wong, W.M., et al. (2005). The use of corticosteroid as treatment in SARS was associated with adverse outcomes: a retrospective cohort study. *J. Infect.* *51*, 98–102.
48. Arabi, Y.M., Mandourah, Y., Al-Hameed, F., Sindi, A.A., Almekhlafi, G.A., Hussein, M.A., Jose, J., Pinto, R., Al-Omari, A., Kharaba, A., et al. (2018). Corticosteroid therapy for critically ill patients with middle east respiratory syndrome. *Am. J. Respir. Crit. Care Med.* *197*, 757–767.
49. Li, H., Chen, C., Hu, F., Wang, J., Zhao, Q., Gale, R.P., and Liang, Y. (2020). Impact of corticosteroid therapy on outcomes of persons with SARS-CoV-2, SARS-CoV, or MERS-CoV infection: a systematic review and meta-analysis. *Leukemia* *34*, 1503–1511.
50. Ding, C., Feng, X., Chen, Y., Yuan, J., Yi, P., Li, Y., Ni, Q., Zou, R., Li, X., Sheng, J., et al. (2020). Effect of corticosteroid therapy on the duration of SARS-CoV-2 clearance in patients with mild COVID-19: a retrospective cohort study. *Infect. Dis. Ther.* *9*, 943–952.
51. Hirano, K., Ichikawa, T., Nakao, K., Matsumoto, A., Miyaaki, H., Shibata, H., Eguchi, S., Takatsuki, M., Ikeda, M., Yamasaki, H., et al. (2008). Differential effects of calcineurin inhibitors, tacrolimus and cyclosporin A, on interferon-induced antiviral protein in human hepatocyte cells. *Liver Transpl.* *14*, 292–298.
52. Carbajo-Lozoya, J., Müller, M.A., Kallies, S., Thiel, V., Drosten, C., and Von Brunen, A. (2012). Replication of human coronaviruses SARS-CoV, HCoV-NL63 and HCoV-229E is inhibited by the drug FK506. *Virus Res.* *165*, 112–117.
53. Alghamdi, M., Mushtaq, F., Awn, N., and Shalhoub, S. (2015). MERS CoV infection in two renal transplant recipients: case report. *Am. J. Transpl.* *15*, 1101–1104.
54. Belli, L.S., Fondevila, C., Cortesi, P.A., Conti, S., Karam, V., Adam, R., Coilly, A., Ericzon, B.G., Loinaz, C., Cuervas-Mons, V., et al. (2020). Protective role of tacrolimus, deleterious role of age and comorbidities in liver transplant recipients with Covid-19: results from the ELITA/ELTR multi-center European study. *Gastroenterology* *160*, 1151–1161.
55. García-Juárez, I., Campos-Murguía, A., Tovar-Méndez, V.H., Gabutti, A., and Ruiz, I. (2020). Unexpected better outcome in a liver transplant recipient with COVID-19: a beneficial effect of tacrolimus? *Rev. Gastroenterol. Mex.* *85*, 437–442.
56. Hayashi, K., Ito, Y., Yamane, R., Yoshizaki, M., Matsushita, K., Kajikawa, G., Kozawa, T., Mizutani, T., Shimizu, Y., Nagano, K., et al. (2021). The case of a liver-transplant recipient with severe acute respiratory syndrome coronavirus 2 infection who had a favorable outcome. *Clin. J. Gastroenterol.* *14*, 842–845.
57. Solanich, X., Antolí, A., Padullés, N., Fanlo-Maresma, M., Iriarte, A., Mitjavila, F., Capdevila, O., Molina, M., Sabater, J., Bas, J., et al. (2021). Pragmatic, open-label, single-center, randomized, phase II clinical trial to evaluate the efficacy and safety of methylprednisolone pulses and tacrolimus in patients with severe pneumonia secondary to COVID-19: the TACROVID trial protocol. *Contemp. Clin. Trials Commun.* *21*. <https://doi.org/10.1101/2021.01.09.21249263>.
58. Sanchez-Pernaute, O., Romero-Bueno, F.I., and Selva-O'Callaghan, A. (2020). Why choose cyclosporin A as first-line therapy in COVID-19 pneumonia. *Reumatol. Clin.* *17*, 555–557.
59. Man, Z., Jing, Z., Huibo, S., Bin, L., and Fanjun, Z. (2020). Viral shedding prolongation in a kidney transplant patient with COVID-19 pneumonia. *Am. J. Transpl.* *20*, 2626–2627.

60. Benotmane, I., Risch, S., Doderer-Lang, C., Caillard, S., and Fafi-Kremer, S. (2021). Long-term shedding of viable SARS-CoV-2 in kidney transplant recipients with COVID-19. *Am. J. Transpl. 21*, 2871–2875.
61. Decker, A., Welzel, M., Laubner, K., Grundmann, S., Kochs, G., Panning, M., Thimme, R., Bode, C., Wagner, D., and Lother, A. (2020). Prolonged SARS-CoV-2 shedding and mild course of COVID-19 in a patient after recent heart transplantation. *Am. J. Transpl. 20*, 3239–3245.
62. Nakajima, Y., Ogai, A., Furukawa, K., Arai, R., Anan, R., Nakano, Y., Kurihara, Y., Shimizu, H., Misaki, T., and Okabe, N. (2021). Prolonged viral shedding of SARS-CoV-2 in an immunocompromised patient. *J. Infect. Chemother. 27*, 387–389.
63. Amini, L., Wagner, D.L., Rössler, U., Zarrinrad, G., Wagner, L.F., Vollmer, T., Wendering, D.J., Kornak, U., Volk, H.D., Reinke, P., et al. (2021). CRISPR-Cas9-Edited tacrolimus-resistant antiviral T cells for advanced adoptive immunotherapy in transplant recipients. *Mol. Ther. 29*, 32–46.
64. Gundry, M.C., Brunetti, L., Lin, A., Mayle, A.E., Kitano, A., Wagner, D., Hsu, J.J., Hoegenauer, K.A., Rooney, C.M., Goodell, M.A., et al. (2016). Highly efficient genome editing of murine and human hematopoietic progenitor cells by CRISPR/Cas9. *Cell Rep. 17*, 1453–1461.
65. Weiskopf, D., Schmitz, K.S., Raadsen, M.P., Grifoni, A., Okba, N.M.A., Endeman, H., van den Akker, J.P.C., Molenkamp, R., Koopmans, M.P.G., van Gorp, E.C.M., et al. (2020). Phenotype and kinetics of SARS-CoV-2-specific T cells in COVID-19 patients with acute respiratory distress syndrome. *Sci. Immunol. 5*, 2071.
66. Shomuradova, A.S., Vagida, M.S., Sheetikov, S.A., Zornikova, K.V., Kiryukhin, D., Titov, A., Peshkova, I.O., Khmelevskaya, A., Dianov, D.V., Malasheva, M., et al. (2020). SARS-CoV-2 epitopes are recognized by a public and diverse repertoire of human T cell receptors. *Immunity 53*, 1245–1257.e5.
67. Bi, J. (2021). CD226: a potent driver of antitumor immunity that needs to be maintained. *Cell. Mol. Immunol.* <https://doi.org/10.1038/s41423-020-00633-0>.
68. Fox, J.C., Nakayama, T., Tyler, R.C., Sander, T.L., Yoshie, O., and Volkman, B.F. (2015). Structural and agonist properties of XCL2, the other member of the C-chemokine subfamily. *Cytokine 71*, 302–311.
69. Tagaya, Y. (2012). P182 Role of IRF8 as a molecular integrator that orchestrates CD8 T effector differentiation. *Cytokine 59*, 578.
70. Savoldo, B., Goss, J.A., Hammer, M.M., Zhang, L., Lopez, T., Gee, A.P., Lin, Y.-F., Quiros-Tejiera, R.E., Reinke, P., Schubert, S., et al. (2006). Treatment of solid organ transplant recipients with autologous Epstein Barr virus-specific cytotoxic T lymphocytes (CTLs). *Blood 108*, 2942.
71. Le Bert, N., Tan, A.T., Kunasegaran, K., Tham, C.Y.L., Hafezi, M., Chia, A., Chng, M.H.Y., Lin, M., Tan, N., Linster, M., et al. (2020). SARS-CoV-2-specific T cell immunity in cases of COVID-19 and SARS, and uninfected controls. *Nature 584*, 457–462.
72. Ren, Y., Shu, T., Wu, D., Mu, J., Wang, C., Huang, M., Han, Y., Zhang, X.Y., Zhou, W., Qiu, Y., et al. (2020). The ORF3a protein of SARS-CoV-2 induces apoptosis in cells. *Cell. Mol. Immunol. 17*, 881–883.
- [73]. Xiong, Y., Liu, Y., Cao, L., Wang, D., Guo, M., Guo, D., et al. (2020). Transcriptomic characteristics of bronchoalveolar lavage fluid and peripheral blood mononuclear cells in COVID-19 patients. *SSRN Electron. J. 9*, 761–770.
74. Oja, A.E., Saris, A., Ghandour, C.A., Kragten, N.A.M., Hogema, B.M., Nossent, E.J., Heunks, L.M.A., Cuvalay, S., Slot, E., Linty, F., et al. (2020). Divergent SARS-CoV-2-specific T- and B-cell responses in severe but not mild COVID-19 patients. *Eur. J. Immunol. 50*, 1998–2012.
75. Zhang, Y., Chen, Y., Li, Y., Huang, F., Luo, B., Yuan, Y., Xia, B., Ma, X., Yang, T., Yu, F., et al. (2021). The ORF8 protein of SARS-CoV-2 mediates immune evasion through down-regulating MHC-I. *Proc. Natl. Acad. Sci. U S A 118*, e2024202118.
76. Peng, Y., Mentzer, A.J., Liu, G., Yao, X., Yin, Z., Dong, D., Dejnirattisai, W., Rostron, T., Supasa, P., Liu, C., et al. (2020). Broad and strong memory CD4+ and CD8+ T cells induced by SARS-CoV-2 in UK convalescent individuals following COVID-19. *Nat. Immunol. 21*, 1336–1345.
77. Gao, Y., Cai, C., Grifoni, A., Müller, T.R., Niessl, J., Olofsson, A., Humbert, M., Hansson, L., Österborg, A., Bergman, P., et al. (2022). Ancestral SARS-CoV-2-specific T cells cross-recognize the Omicron variant. *Nat. Med. 2022*, 1–9.
78. Jordan, S.C., Shin, B.H., Gadsden, T.A.M., Chu, M., Petrosyan, A., Le, C.N., Zabner, R., Oft, J., Pedraza, I., Cheng, S., et al. (2021). T cell immune responses to SARS-CoV-2 and variants of concern (Alpha and Delta) in infected and vaccinated individuals. *Cell. Mol. Immunol. 18*, 2554–2556.
79. Geers, D., Shamier, M.C., Bogers, S., den Hartog, G., Gommers, L., Nieuwkoop, N.N., Schmitz, K.S., Rijsbergen, L.C., van Osch, J.A.T., Dijkhuizen, E., et al. (2021). SARS-CoV-2 variants of concern partially escape humoral but not T-cell responses in COVID-19 convalescent donors and vaccinees. *Sci. Immunol. 6*, eabj1750.
80. Mateus, J., Grifoni, A., Tarke, A., Sidney, J., Ramirez, S.L., Dan, J.M., Burger, Z.C., Rawlings, S.A., Smith, D.M., Phillips, E., et al. (2020). Selective and cross-reactive SARS-CoV-2 T cell epitopes in unexposed humans. *Science 70*, 89–94.
81. Grifoni, A., Voic, H., Dhanda, S.K., Kidd, C.K., Brien, J.D., Buus, S., Stryhn, A., Durbin, A.P., Whitehead, S., Diehl, S.A., et al. (2020). T cell responses induced by attenuated flavivirus vaccination are specific and show limited cross-reactivity with other flavivirus species. *J. Virol. 94*, e00089–20.
82. Ferretti, A.P., Kula, T., Wang, Y., Bertino, S.A., Chattopadhyay, S., and Correspondence, G.M. (2020). Unbiased Screens Show CD8+ T Cells of COVID-19 Patients Recognize Shared Epitopes in SARS-CoV-2 that Largely Reside outside the Spike Protein. *Immunity 53*, 1095–1107.
83. Stervbo, U., Rahmann, S., Roch, T., Westhoff, T.H., and Babel, N. (2020). Epitope similarity cannot explain the pre-formed T cell immunity towards structural SARS-CoV-2 proteins. *Sci. Rep. 10*, 18995.
84. Lipsitch, M., Grad, Y.H., Sette, A., and Crotty, S. (2020). Cross-reactive memory T cells and herd immunity to SARS-CoV-2. *Nat. Rev. Immunol. 20*, 709–713.
85. Channappanavar, R., Zhao, J., and Perlman, S. (2014). T cell-mediated immune response to respiratory coronaviruses. *Immunol. Res. 59*, 118–128.
86. Okhrimenko, A., Grün, J.R., Westendorf, K., Fang, Z., Reinke, S., Von Roth, P., Wassilew, G., Kühn, A.A., Kudernatsch, R., Demski, S., et al. (2014). Human memory T cells from the bone marrow are resting and maintain long-lasting systemic memory. *Proc. Natl. Acad. Sci. U S A 111*, 9229–9234.
87. Walton, S., Mandaric, S., and Oxenius, A. (2013). CD4 T cell responses in latent and chronic viral infections. *Front. Immunol. 4*, 105.
88. Amini, L., Vollmer, T., Wendering, D.J., Jurisch, A., Landwehr-Kenzel, S., Otto, N.M., Jürchott, K., Volk, H.D., Reinke, P., and Schmüeck-Hennesse, M. (2019). Comprehensive characterization of a next-generation antiviral T-cell product and feasibility for application in immunosuppressed transplant patients. *Front. Immunol. 10*, 1148.
89. Neideman, J., Luo, X., Frouard, J., Xie, G., Gill, G., Stein, E.S., McGregor, M., Ma, T., George, A.F., Kosters, A., et al. (2020). SARS-CoV-2-Specific T cells exhibit phenotypic features of helper function, lack of terminal differentiation, and high proliferation potential. *Cell Rep. Med 1*, 100081.
90. Powell, D.J., Dudley, M.E., Robbins, P.F., and Rosenberg, S.A. (2005). Transition of late-stage effector T cells to CD27+ CD28+ tumor-reactive effector memory T cells in humans after adoptive cell transfer therapy. *Blood 105*, 241–250.
91. Gattinoni, L., Klebanoff, C.A., Palmer, D.C., Wrzesinski, C., Kerstann, K., Yu, Z., Finkelstein, S.E., Theoret, M.R., Rosenberg, S.A., and Restifo, N.P. (2005). Acquisition of full effector function in vitro paradoxically impairs the in vivo antitumor efficacy of adoptively transferred CD8+ T cells. *J. Clin. Invest. 115*, 1616–1626.
92. Verma, K., Ogonek, J., Varanasi, P.R., Luther, S., Bünting, I., Thomay, K., Behrens, Y.L., Mischak-Weissinger, E., and Hambach, L. (2017). Human CD8+ CD57-TEMRA cells: too young to be called “old. *PLoS One 12*, e0177405.
93. Rufer, N., Zippelius, A., Batard, P., Pittet, M.J., Kurth, I., Corthesy, P., Cerottini, J.C., Leyvraz, S., Roosnek, E., Nabholz, M., et al. (2003). Ex vivo characterization of human CD8+ T subsets with distinct replicative history and partial effector functions. *Blood 102*, 1779–1787.
94. Youngblood, B., Hale, J.S., Kissick, H.T., Ahn, E., Xu, X., Wieland, A., Araki, K., West, E.E., Ghoneim, H.E., Fan, Y., et al. (2017). Effector CD8 T cells dedifferentiate into long-lived memory cells. *Nature 552*, 404–409.
95. Schmüeck, M., Fischer, A.M., Hammoud, B., Brestrich, G., Fuehrer, H., Luu, S.-H., Mueller, K., Babel, N., Volk, H.-D., and Reinke, P. (2012). Preferential expansion of human virus-specific multifunctional central memory T cells by partial targeting of

- the IL-2 receptor signaling pathway: the key role of CD4 + T cells. *J. Immunol.* *188*, 5189–5198.
96. Strauss, G., Osen, W., and Debatin, K.M. (2002). Induction of apoptosis and modulation of activation and effector function in T cells by immunosuppressive drugs. *Clin. Exp. Immunol.* *128*, 255–266.
  97. Imai, A., Sahara, H., Tamura, Y., Jimbow, K., Saito, T., Ezo, K., Yotsuyanagi, T., and Sato, N. (2007). Inhibition of endogenous MHC class II-restricted antigen presentation by tacrolimus (FK506) via FKBP51. *Eur. J. Immunol.* *37*, 1730–1738.
  98. Lee, Y.R., Yang, I.H., Lee, Y.H., Sun, A., Song, S., Li, H., Han, K., Kim, K., Eo, S.K., and Lee, C.K. (2005). Cyclosporin A and tacrolimus, but not rapamycin, inhibit MHC-restricted antigen presentation pathways in dendritic cells. *Blood* *105*, 3951–3955.
  99. Viola, A., and Lanzavecchia, A. (1996). T cell activation determined by T cell receptor number and tunable thresholds. *Science* *273*, 104–106.
  100. Danese, S., Sans, M., and Fiocchi, C. (2004). The CD40/CD40L costimulatory pathway in inflammatory bowel disease. *Gut* *53*, 1035.
  101. Moens, L., and Tangye, S.G. (2014). Cytokine-mediated regulation of plasma cell generation: IL-21 takes center stage. *Front. Immunol.* *5*, 65.
  102. Duvall, M.G., Precopio, M.L., Ambrozak, D.A., Jaye, A., McMichael, A.J., Whittle, H.C., Roederer, M., Rowland-Jones, S.L., and Koup, R.A. (2008). Polyfunctional T cell responses are a hallmark of HIV-2 infection. *Eur. J. Immunol.* *38*, 350–363.
  103. Harari, A., Vallelian, F., Meylan, P.R., and Pantaleo, G. (2005). Functional heterogeneity of memory CD4 T cell responses in different conditions of antigen exposure and persistence. *J. Immunol.* *174*, 1037–1045.
  104. Silva-Filho, J.L., Caruso-Neves, C., and Pinheiro, A.A.S. (2014). IL-4: an important cytokine in determining the fate of T cells. *Biophys. Rev.* *6*, 111–118.
  105. Zimmerli, S.C., Harari, A., Cellerai, C., Vallelian, F., Bart, P.A., and Pantaleo, G. (2005). HIV-1-specific IFN- $\gamma$ /IL-2-secreting CD8 T cells support CD4-independent proliferation of HIV-1-specific CD8 T cells. *Proc. Natl. Acad. Sci. U S A* *102*, 7239–7244.
  106. Batista, N.V., Chang, Y.-H., Chu, K.-L., Wang, K.C., Girard, M., and Watts, T.H. (2020). T cell-intrinsic CX3CR1 marks the most differentiated effector CD4 + T cells, but is largely dispensable for CD4 + T cell responses during chronic viral infection. *ImmunoHorizons* *4*, 701–712.
  107. Sacre, K., Hunt, P.W., Hsue, P.Y., Maidji, E., Martin, J.N., Deeks, S.G., Autran, B., and McCune, J.M. (2012). A role for cytomegalovirus-specific CD4 +CX3CR1 + T cells and cytomegalovirus-induced T-cell immunopathology in HIV-associated atherosclerosis. *AIDS* *26*, 805–814.
  108. Ding, Z.C., Liu, C., Cao, Y., Habetsion, T., Kuczma, M., Pi, W., Kong, H., Cacan, E., Greer, S.F., Cui, Y., et al. (2016). IL-7 signaling imparts polyfunctionality and stemness potential to CD4+ T cells. *Oncoimmunology* *5*, e1171445.
  109. Cannarile, M.A., Lind, N.A., Rivera, R., Sheridan, A.D., Camfield, K.A., Wu, B.B., Cheung, K.P., Ding, Z., and Goldrath, A.W. (2006). Transcriptional regulator Id2 mediates CD8+ T cell immunity. *Nat. Immunol.* *7*, 1317–1325.
  110. Lee, J., Su, E.W., Zhu, C., Hainline, S., Phuah, J., Moroco, J.A., Smithgall, T.E., Kuchroo, V.K., and Kane, L.P. (2011). Phosphotyrosine-dependent coupling of tim-3 to T-cell receptor signaling pathways. *Mol. Cell. Biol.* *31*, 3963–3974.
  111. Chen, X., Woiciechowsky, A., Raffegerst, S., Schendel, D., Kolb, H.-J., and Roskrow, M. (2000). Impaired expression of the CD3-zeta chain in peripheral blood T cells of patients with chronic myeloid leukaemia results in an increased susceptibility to apoptosis. *Br. J. Haematol.* *111*, 817–825.
  112. Khan, O., Giles, J.R., McDonald, S., Manne, S., Ngoi, S.F., Patel, K.P., Werner, M.T., Huang, A.C., Alexander, K.A., Wu, J.E., et al. (2019). TOX transcriptionally and epigenetically programs CD8+ T cell exhaustion. *Nature* *571*, 211–218.
  113. Li, J., He, Y., Hao, J., Ni, L., and Dong, C. (2018). High levels of eomes promote exhaustion of anti-tumor CD8+ T cells. *Front. Immunol.* *9*, 2981.
  114. Cameron, A.M., Steiner, J.P., Sabatini, D.M., Kaplin, A.I., Walensky, L.D., and Snyder, S.H. (1995). Immunophilin FK506 binding protein associated with inositol 1,4,5-trisphosphate receptor modulates calcium flux. *Proc. Natl. Acad. Sci. U S A* *92*, 1784–1788.
  115. Wherry, E.J., and Kurachi, M. (2015). Molecular and cellular insights into T cell exhaustion. *Nat. Rev. Immunol.* *15*, 486–499.
  116. Zhang, Y., Baysac, K.C., Yee, L.F., Saporita, A.J., and Weber, J.D. (2014). Elevated DDX21 regulates c-Jun activity and rRNA processing in human breast cancers. *Breast Cancer Res.* *16*, 1–18.
  117. Audrito, V., Messana, V.G., and Deaglio, S. (2020). NAMPT and NAPRT: two metabolic enzymes with key roles in inflammation. *Front. Oncol.* *10*, 358.
  118. Vester, S.K., Beavil, R.L., Lynham, S., Beavil, A.J., Cunninghame Graham, D.S., McDonnell, J.M., and Vyse, T.J. (2021). Nucleolin acts as the receptor for C1QTNF4 and supports C1QTNF4-mediated innate immunity modulation. *J. Biol. Chem.* *296*, 100513.
  119. Toriyama, K., Kuwahara, M., Kondoh, H., Mikawa, T., Takemori, N., Konishi, A., Yorozuya, T., Yamada, T., Soga, T., Shiraishi, A., et al. (2020). T cell-specific deletion of Pgam1 reveals a critical role for glycolysis in T cell responses. *Commun. Biol.* *3*, 394.
  120. Luo, D., Wang, G., Shen, W., Zhao, S., Zhou, W., Wan, L., Yuan, L., Yang, S., and Xiang, R. (2016). Clinical significance and functional validation of PPA1 in various tumors. *Cancer Med.* *5*, 2800.
  121. Stinchcombe, J.C., Barral, D.C., Mules, E.H., Booth, S., Hume, A.N., Machesky, L.M., Seabra, M.C., and Griffiths, G.M. (2001). Rab27a is required for regulated secretion in cytotoxic T lymphocytes. *J. Cell Biol.* *152*, 825.
  122. Brestrich, G., Zwinger, S., Roemhild, A., Noutsias, M., Rohde, M., Keeren, K., Sawitzki, B., Volk, H.D., Reinke, P., and Hammer, M.H. (2009). Generation of HCMV-specific T-cell lines from seropositive solid-organ-transplant recipients for adoptive T-cell therapy. *J. Immunother.* *32*, 932–940.
  123. Berar Yanay, N. (2021). Low immunization rates among kidney transplant recipients who received 2 doses of the mRNA-1273 SARS-CoV-2 vaccine. *Kidney Int.* *99*, 1498–1500.
  124. Vakulskas, C.A., Dever, D.P., Rettig, G.R., Turk, R., Jacobi, A.M., Collingwood, M.A., Bode, N.M., McNeill, M.S., Yan, S., Camarena, J., et al. (2018). A high-fidelity Cas9 mutant delivered as a ribonucleoprotein complex enables efficient gene editing in human hematopoietic stem and progenitor cells. *Nat. Med.* *24*, 1216–1224.
  125. Moosmann, A., Khan, N., Cobbold, M., Zentz, C., Delecluse, H.J., Hollweck, G., Hislop, A.D., Blake, N.W., Croom-Carter, D., Wollenberg, B., et al. (2002). B cells immortalized by a mini-Epstein-Barr virus encoding a foreign antigen efficiently reactivate specific cytotoxic T cells. *Blood* *100*, 1755–1764.
  126. Hammoud, B., Schmuck, M., Fischer, A.M., Fuehrer, H., Park, S.J., Akyuz, L., Schefold, J.C., Raftery, M.J., Schönrich, G., Kaufmann, A.M., et al. (2013). HCMV-specific T-cell therapy: do not forget supply of help. *J. Immunother.* *36*, 93–101.
  127. Hermans, I.F., Silk, J.D., Yang, J., Palmowski, M.J., Gileadi, U., McCarthy, C., Salio, M., Ronchese, F., and Cerundolo, V. (2004). The VITAL assay: a versatile fluorometric technique for assessing CTL- and NKT-mediated cytotoxicity against multiple targets in vitro and in vivo. *J. Immunol. Methods* *285*, 25–40.
  128. Daneshgar, A., Klein, O., Nebrich, G., Weinhart, M., Tang, P., Arnold, A., Ullah, I., Pohl, J., Moosburner, S., Raschok, N., et al. (2020). The human liver matrisome - Proteomic analysis of native and fibrotic human liver extracellular matrices for organ engineering approaches. *Biomaterials* *257*, 120247.
  129. Ferreira-Gomes, M., Kruglov, A., Durek, P., Heinrich, F., Tizian, C., Heinz, G.A., Pascual-Reguant, A., Du, W., Mothes, R., Fan, C., et al. (2021). SARS-CoV-2 in severe COVID-19 induces a TGF- $\beta$ -dominated chronic immune response that does not target itself. *Nat. Commun.* *12*, 1–14.
  130. Lun, A.T.L., McCarthy, D.J., and Marioni, J.C. (2016). A step-by-step workflow for low-level analysis of single-cell RNA-seq data with Bioconductor [version 2; peer review: 3 approved, 2 approved with reservations]. *F1000Res.* *5*, 2122.
  131. Borcherding, N., and Bormann, N.L. (2020). scRepertoire: an R-based toolkit for single-cell immune receptor analysis [version 2; peer review: 2 approved]. *F1000Res.* *9*, 47.